INVESTIGATION OF THE EMISSION PROPERTIES OF QUANTUM DOT-THERMORESPONSIVE POLYMER NANOCOMPOSITE HYDROGELS WITH TEMPERATURE

A Thesis

by

AMEET RAJKUMAR JURIANI

Submitted to the Office of Graduate Studies of
Texas A&M University
in partial fulfillment of the requirements for the degree of

MASTER OF SCIENCE

May 2010

Major Subject: Biomedical Engineering

INVESTIGATION OF THE EMISSION PROPERTIES OF QUANTUM DOT-THERMORESPONSIVE POLYMER NANOCOMPOSITE HYDROGELS WITH TEMPERATURE

A Thesis

by

AMEET RAJKUMAR JURIANI

Submitted to the Office of Graduate Studies of
Texas A&M University
in partial fulfillment of the requirements for the degree of

MASTER OF SCIENCE

Approved by:

Co-Chairs of Committee,	Kenith E. Meissner
	Rainer Fink
Committee Member,	Melissa A. Grunlan
Head of Department,	Gerard L. Cote

May 2010

Major Subject: Biomedical Engineering

ABSTRACT

Investigation of the Emission Properties of Quantum Dot-Thermoresponsive Polymer Nanocomposite Hydrogels with Temperature.

(May 2010)

Ameet Rajkumar Juriani, B.E., Mumbai University

Co-Chairs of Advisory Committee: Dr. Kenith E. Meissner
Dr. Rainer Fink

This thesis presents a novel method for the preparation of quantum dot-thermoresponsive polymer nanocomposite hydrogels. The quantum dots (QD's) were synthesized in a microwave reactor using a high temperature organometallic synthesis procedure. The initial hydrophobic surface layer on the QD's was coated with an amphiphilic polymer to enable phase transfer from non-polar solvent to water followed by physical immobilization of the QD's in the thermoresponsive polymer hydrogel by photopolymerization. Their temperature dependent emission properties were investigated as a function of concentration of the incorporated QD's. The resultant temperature dependent changes in the position of the peak emission wavelength of the QD-polymer nanocomposite hydrogels were found to be due to the change in the physical environment causing increased interaction between the embedded amphiphilic polymer coated QD's and/or due to aggregation of QD's. This change in peak emission position was found to be reversible in the temperature range from 29 to 37 °C.

DEDICATION

I dedicate this work to my loving family: my parents, Rajkumar and Geeta, and my brother and sister-in-law, Sumeet and Hema, for all their love and support.

ACKNOWLEDGEMENTS

I would like to thank my advisor and mentor, Dr. Kenith Meissner, for all his support, patience and constant encouragement throughout my graduate studies. The knowledge and experience I gained under his guidance will truly remain an invaluable asset to me. I would also like to express my sincere gratitude towards my co-chair, Dr. Rainer Fink, and my committee member, Dr. Melissa Grunlan, for their guidance and support throughout the course of this research.

I am grateful to Dr. Amanda Young and Dr. Christos Savva for the help and training they imparted to me on some of the characterization instruments actively used in this research.

I wish to thank former and present members of our group, Bhavik Nathwani, Clark Needham, Kyle Borque, Shuo Pang, Hope Beier, Ravish Majithia, Sina Amini and Sarah Jeffords, for all their help and encouragement. Thanks to all of my friends who made learning at Texas A&M University a great experience.

Finally, special heartfelt thanks to my best friend, Swati Goyal; she always stood beside me like a rock during my good and bad times.

NOMENCLATURE

BIS	*N, N'*-methylenebisacrylamide
CdO	Cadmium Oxide
CdSe	Cadmium Selenide
CdTe	Cadmium Telluride
DI	Deionized
DMZ	Dimethylzinc
FRET	Förster Resonance Energy Transfer
FWHM	Full Width at Half Maximum
FWTM	Full Width at Tenth Maximum
HC	High Concentration
HMDS	Hexamethyldisilathiane
IR	Infrared
LC	Low Concentration
LCST	Lower Critical Solution Temperature
LED's	Light Emitting Diodes
MC	Medium Concentration
MW	Microwave
NIPAM	*N*-isopropylacrylamide
PEI	Polyethylenemine
PL	Photoluminescent

PMMA	Poly(methyl methacrylate)
Poly(NIPAM)	Poly(*N*-isopropylacrylamide)
PNIPAM	Poly(*N*-isopropylacrylamide)
QD's	Quantum Dots
RPM	Rotations per Minute
RT	Room Temperature
Se	Selenium
T	Temperature
TDPA	Tetradecylphosphonic Acid
TEM	Transmission Electron Microscope
TOP	Tri-*n*-octylphosphine
TOPO	Tri-*n*-octylphosphine Oxide
UV	Ultra Violet
ZnS	Zinc Sulfide

TABLE OF CONTENTS

CHAPTER Page

LIST OF FIGURES

FIGURE Page

FIGURE Page

LIST OF TABLES

CHAPTER I

INTRODUCTION AND MOTIVATION

Luminescent semiconductor nanocrystals, or quantum dots (QD's) have gained increasing attention from researchers for their unique optical and electrical characteristics due to quantum confinement effects [1]. High luminescence, near Gaussian narrow emission, broad absorption band and resistance to photobleaching are some of the attractive properties which render QD's suitable for a variety of technological applications ranging from biomarkers [2, 3], light emitting diodes (LED's) [4, 5], solar cells [6] and optical sensing [7, 8].

Pioneering work by Murray et al. [9] on colloidal synthesis of monodisperse, size tunable type II-IV QD's followed by significant improvements by Hines et al. [10] and Peng et al. [11] made QD synthesis in laboratory feasible. These synthesis methods were based on organometallic pyrolysis of precursors which often required heating at temperatures up to 300 °C. There were several disadvantages associated with the conventional heating methods employed; this affected the quality of the synthesized QD's.

This thesis follows the style of Biomaterials.

Microwave (MW) assisted synthesis procedures gradually emerged as an alternative route for efficient QD synthesis [12, 13]. Commercially available MW reactors specifically designed for chemical synthesis and equipped with advanced control features enabled optimization of existing QD synthesis methods leading to precise control of the reaction parameters, faster reaction rates and synthesis of nearly monodisperse QD samples with high photoluminescent (PL) intensity. Thus, implementation of a MW based system for QD synthesis was considered favorable. This report discusses in detail the implementation of the system, methodology and the procedure followed for synthesis of QD's in a MW reactor.

Nanothermometry finds numerous applications in the areas of biotechnology, biosensors and bioMEMS. Various approaches have been devised and developed for effective temperature measurement at the nanoscale [14]. Optical nanothermometry using QD's is one such approach. Efforts have been made to use luminescent QD's as standalone optical temperature probes [8, 15]. When incorporated in thermoresponsive polymers such as poly(*N*-isopropylacrylamide), the emission properties of QD's have shown strong dependence with varying temperature [16]. Poly(*N*-isopropylacrylamide) also popularly known as poly(NIPAM) or PNIPAM exhibits a temperature dependent phase transition phenomenon and switches from being hydrophilic to hydrophobic and vice-versa, in aqueous solution [17]. Thus, when optical properties of QD's are effectively combined with the physical properties of thermoresponsive polymers, they can serve as building blocks for optical nanothermometers.

In this work, cadmium selenide/zinc sulfide (CdSe/ZnS) core-shell QD's coated with an amphiphilic polymer were incorporated in poly(NIPAM) hydrogels. The temperature dependent emission spectra of the hydrogels were then recorded as a function of the concentration of the incorporated QD's. This work has a potential to serve as a useful guideline in providing a comprehensive understanding of the feasibility of developing QD-thermoresponsive polymer nanocomposite hydrogel based optical temperature sensors.

CHAPTER II

BACKGROUND

This chapter explains the implementation of a MW based system for synthesis of QD's. It also discusses the general characteristics of poly(*N*-isopropylacrylamide) thermoresponsive polymer and the temperature dependent behavior of QD-thermoresponsive polymer nanocomposite hydrogels.

2.1 Heating methods for synthesis of QD's

Conventional heating methods such as convective and conductive heating have been a primary choice of QD researchers for high temperature initiated QD synthesis. Heated oil bath, heating mantle and sand bath are some of the previously utilized heating methods [18-22]. A major disadvantage of these methods is that the temperature on the outside surface of the reaction vessel is greater than the internal temperature. The reaction vessel acts as an intermediary for energy transfer from the heating source to the solvent and finally to the reactant molecules. This results in acute thermal gradients through the bulk solution causing non-uniform heating conditions [12] (Figure 1). Also, due to indirect method of heat transfer it is a time consuming process with limited control over the reaction parameters. Specifically for QD synthesis, precise control of the reaction parameters such as nucleation time and reaction temperature is a key factor for controlling the growth (size) of the nanocrystals and hence their emission wavelength.

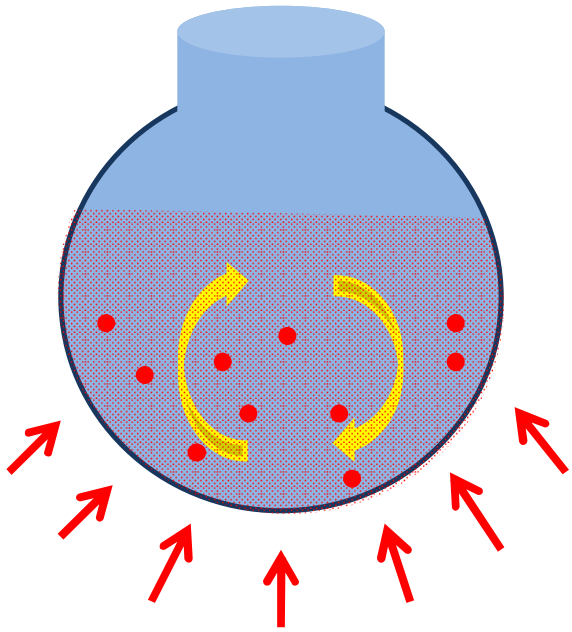

Figure 1. Schematic representation of conventional heating for QD synthesis.

On the other hand, MW's in the form of domestic household microwave ovens have been used as a reliable heating source in the kitchen for many years. It was not until recently that MW technology gained tremendous impetus for organic synthesis purposes. With advances in MW assisted QD synthesis chemistry, MW's have gradually emerged as an alternative energy source for QD synthesis [23]. MW's are powerful enough to accomplish chemical transformations in a much quicker and energy efficient manner as compared to conventional heating methods. Energy is transferred rapidly and directly through the glass reaction vessel to the MW absorbing materials which bring about localized superheating of the reactant molecules (Figure 2).

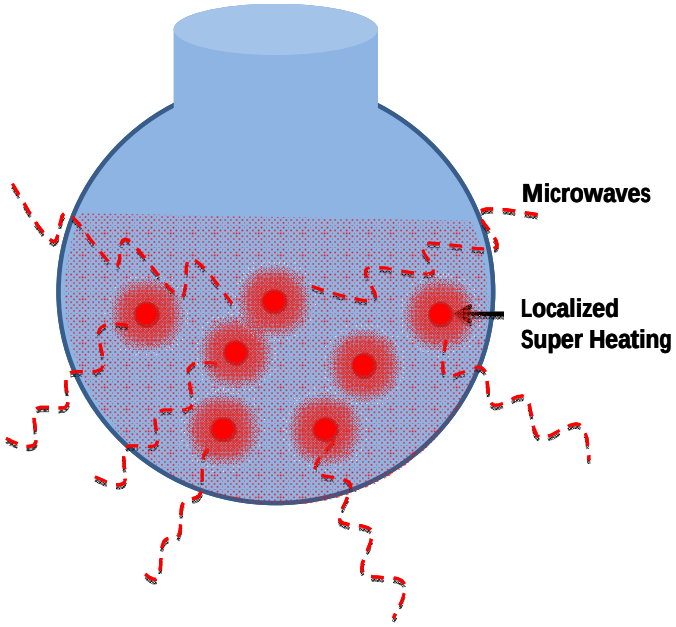

Figure 2. Schematic representation of microwave heating for QD synthesis.

Researchers have considered the idea of using modified domestic MW ovens for organic synthesis [24, 25]. In a domestic MW, the MW's are generated as pulses of electromagnetic (EM) radiation which get reflected from the cavity walls (Figure 3). The EM field produced is inhomogeneous and leads to the formation of hot and cold spots in the reaction vessel. It is also hard to determine the reaction temperature in an accurate and reliable way. Another major drawback of these retrofitted household appliances is lack of proper control systems. Safety is a major concern as heating of organic solvents in open vessels inside a MW oven may lead to explosions or pose a serious fire hazard induced by electric arcs inside the cavity due to continuous switching of the magnetron.

These shortcomings lead to the need of a dedicated instrument designed of chemical synthesis.

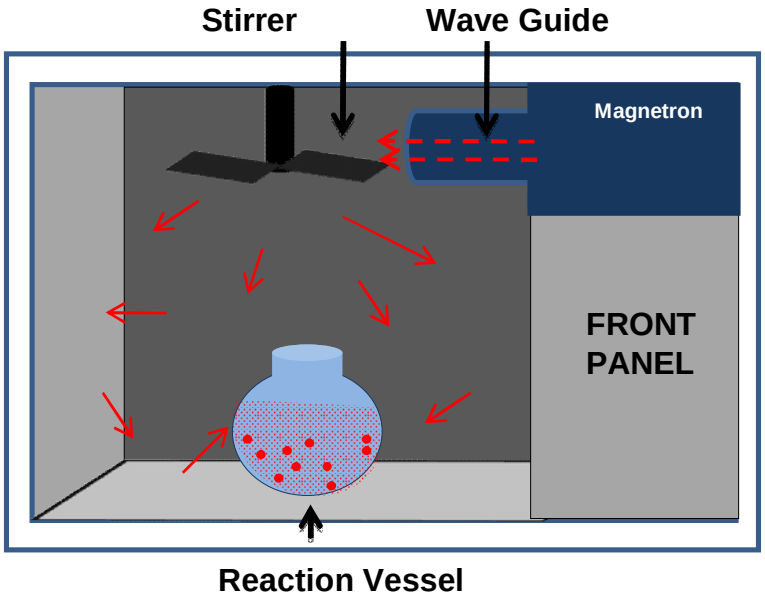

Figure 3. Schematic representation of multimode cavity in a domestic microwave.

Commercially available MW reactors specially designed for chemical synthesis allow precise control of essential reaction parameters such as the applied MW power, reaction temperature, reaction time and in some cases internal vessel pressure [26]. In these instruments MW's are generated as continuous EM waves as opposed to pulses. These EM waves are then transferred through a waveguide to the reaction vessel mounted at a fixed distance from the irradiating source (Figure 4). This creates a standing wave and as a result the EM field is homogenous leading to uniform heating of the reaction vessel and hence the reactant molecules.

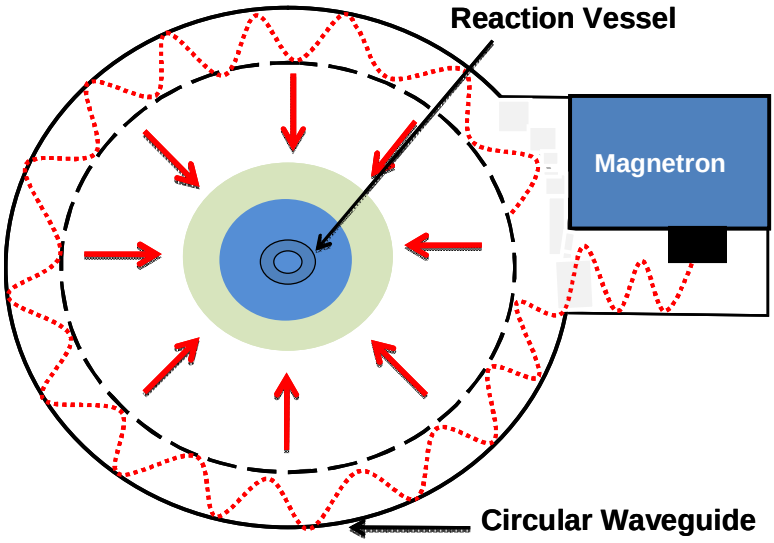

Figure 4. Schematic representation of single mode cavity in a microwave reactor.

2.2 Implementation of MW based system for synthesis of QD's

CdSe/ZnS core-shell QD's are synthesized in our laboratory by high temperature organometallic synthesis procedure. Previously, heating was carried out in a metal bath reactor containing an alloy of bismuth with a melting point of 110 °C (Figure 5). Temperature of the metal bath was measured using a thermocouple probe connected to a feedback controller with a digital read out. A standard drill press connected to a variable autotransformer was modified to act as a stirrer mechanism. The reaction time and temperature had to be controlled manually by lowering down and lifting up the glass reaction vessel inside the metal bath during the course of synthesis reaction.

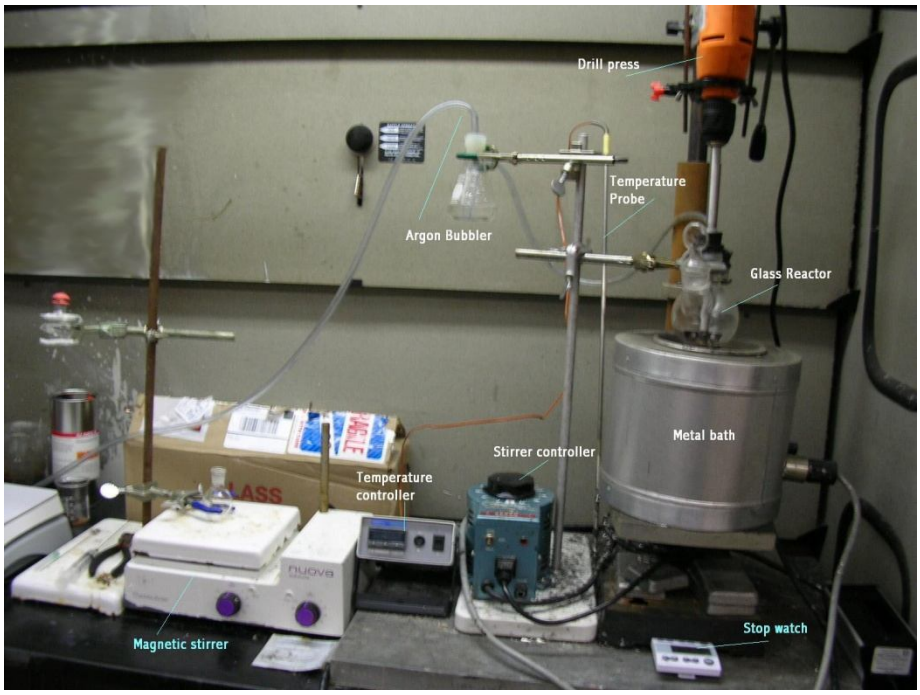

Figure 5. Experimental setup for QD synthesis in metal bath reactor.

Disadvantages of metal bath reactor QD synthesis system: (1) time consuming and labor intensive; (2) lack of control over the synthesis process; (3) lack of reproducibility of reaction results; (4) energy inefficient and (5) potential safety hazard due to molten metal at high temperature.

To address these issues implementation of a MW based system for QD synthesis was advantageous. A commercially available MW reactor was purchased from CEM Corporation, NC. The 'Discover®- BenchMate' series of MW reactor provided versatility and simplicity of operation for carrying out synthesis of QD's under laboratory conditions. It was equipped with single mode MW cavity with maximum power rating of 300 W. It had a built in magnetic stirrer mechanism and an infrared (IR)

probe for accurate and contact less temperature measurement. This instrument provided us with a convenient way of dynamically controlling the synthesis reaction with the help of a bundled computer software program (Figure 6).

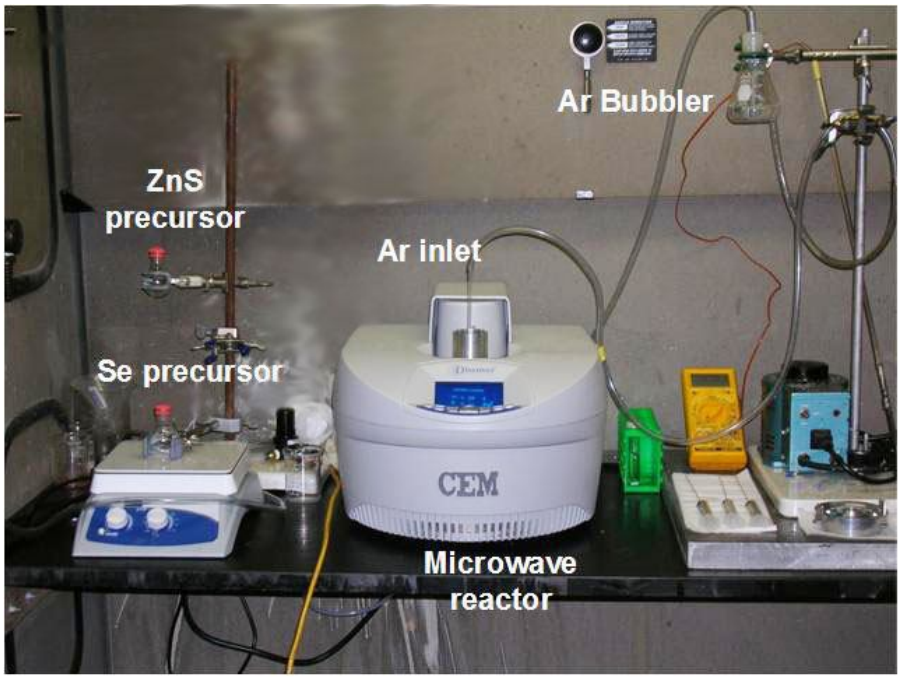

Figure 6. Experimental setup for QD synthesis in microwave reactor.

Advantages of MW based QD synthesis system: (1) time saving with minimum human intervention; (2) better control over the synthesis process; (3) better quality final product and possible to achieve reproducible results; (4) safe method for QD synthesis and (5) energy efficient.

Figure 7 shows a visual comparison of the QD synthesis reaction performed using a metal bath reactor and a MW reactor. In case of a metal bath reactor the dark

appearance of the supernatant is due to excessive heating of the coordinating solvent caused due to indirect method of energy transfer. This was absent in case of a MW based reactor as the supernatant is colorless and clear. The energy is transferred directly for a shorter period of time and there is no unnecessary overheating of the coordinating solvent. Post synthesis, QD's are washed with methanol to remove the excess coordinating solvent and unreacted precursors. Due to charring of the coordinating solvent in a metal bath reactor the synthesized QD's have to be washed twice as more compared to two methanol washes in a MW reactor. Excessive washing causes loss of QD's thus decreasing the overall mass yield of the synthesis reaction. As a result, QD's synthesized in a MW reactor can be easily recovered with less number of methanol washes as compared to when synthesized in a metal bath reactor.

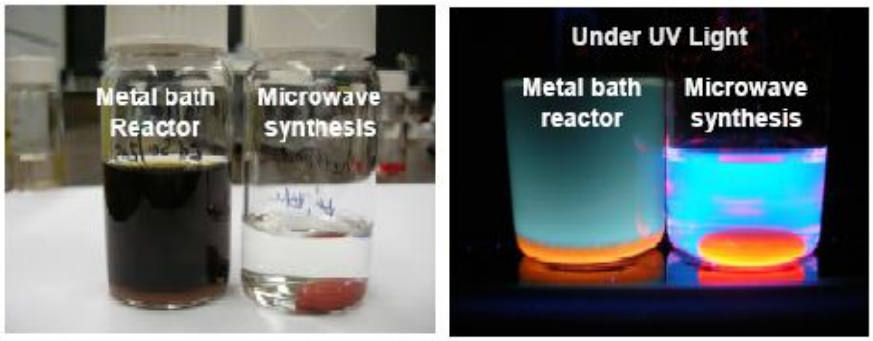

Figure 7. Metal bath reactor vs. microwave reactor seen in ambient light (L) and seen in UV light (R).

2.3 Temperature dependent emission properties of QD's

Luminescent properties of QD's are temperature dependent and therefore widely studied for potential applications as optical temperature indicators. Bawendi and co-workers showed that the steady state PL properties of CdSe/ZnS QD's dispersed in a poly(laural-methacrylate) (PLMA) matrix were strongly dependent on temperature in the range from 100 to 315 K (-173.15 to 41.85 °C). It was reported that the peak emission shifts to shorter wavelength accompanied by significant increase in the PL intensity with decreasing temperature [15]. Further; this change in the PL intensity was reported to be reversible with temperature. This phenomenon can be well explained by the band gap variation of the nanoscale semiconductor material with temperature. In case of CdSe QD's in the temperature range from 235 to 385 K (-38.15 to 111.85 °C), an increase in temperature results in a size dependent decrease of the band gap which in turn causes the peak emission to exhibit a red shift [27]. In another approach, CdTe QD's were deposited on optical fibers by layer-by-layer electrostatic self-assembly method to act as optical temperature sensors. These sensors showed a linear and reversible variation of the emission wavelength in the temperature range from 30 to 100 °C [8].

2.4 Temperature sensitive polymers

Thermoresponsive polymers fall under the category of "smart" polymers. They undergo a physical or chemical change in response to external stimuli, such as temperature. Some of the commonly known thermoresponsive polymers are PIOZ - poly(2-isopropyl-2-oxazoline), PVCL - poly(*N*-vinylcaprolactam), PDEAAM -

poly(*N*,*N*,-diethylacrylamide) and PNIPAM - poly(*N*-isopropylacrylamide) [28]. One important parameter of these polymers is their lower critical solution temperature (LCST) where the polymer undergoes phase transformation in response to change in temperature. For example, poly(NIPAM) thermoresponsive polymer (Figure 8) has its LCST closest to the body temperature, approximately 32 °C, which makes it suitable for biomedical applications. Poly(NIPAM) is hydrophilic at temperatures below LCST and hydrophobic at temperatures above LCST; in other words it undergoes a reversible thermoresponsive phase transition across the LCST [29] (Figure 9). This can be explained by the ability of poly(NIPAM) to undergo reversible formation and cleavage of hydrogen bonds between its monomer side groups and the surrounding water molecules. As a result, poly(NIPAM) undergoes changes in conformation during the phase transition regime. This property of PNIPAM polymers has been utilized for controlled release of cells [30, 31] and controlled drug delivery applications [32].

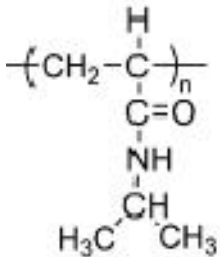

Figure 8. Chemical structure of poly(NIPAM) [28].

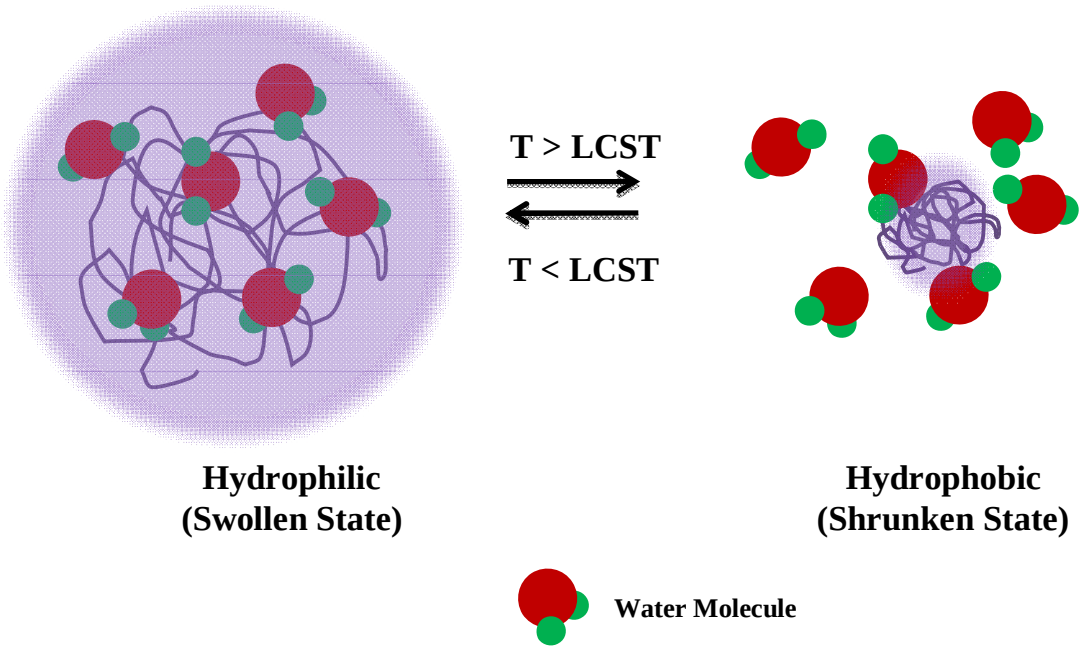

Figure 9. Schematic illustration of temperature induced phase transition in poly(NIPAM).

2.5 QD-thermoresponsive polymer nanocomposite hydrogels

Spectral properties of QD's depend to some extent upon their surrounding environment. Their overall behavior can be altered by changing the physical environment in which they exist. Thus, embedding QD's in smart polymer matrices may be an efficient way of enhancing their functionality [33]. Gong and coworkers constructed luminescent microspheres by incorporating thioglycerol and thioglycolic acid capped CdTe QDs in poly(NIPAM) [34]. Their results indicated that there exists a hydrogen bond between the ligands capped on CdTe QD's and the poly(NIPAM) chains. They also attempted to study the FRET effect between QD's by loading two different sizes of TGA/TGOL capped CdTe QDs embedded in poly(NIPAM) spheres. In a similar

approach, Li and coworkers used poly(NIPAM) hydrogels as a solid matrix for the physical immobilization of aqueous CdTe QD's [16]. It was reported that PL intensity of the nanocomposite gels decreased with increase in temperature accompanied by a linear red shift (~ 13 nm) of the PL maximum wavelengths in the temperature range from 25 to 41 °C. Also, it was reported that the changes in the PL peak wavelengths due to temperature were reversible. According to the authors the possible reason for the observed red shift may be energy transfer between close packed CdTe QD's at temperatures across the LCST. But, they had failed to report or consider the concentration of the QD's inside the hydrogel; this information would have helped validate their claim of energy transfer between close packed QD's inside the hydrogel. With the concentration information it would have been possible to estimate the approximate number of QD's in the given volume and the average the inter dot spacing between them. This was necessary as energy transfer between two fluorophores greatly depends upon the spacing between them [35].

In this work, amphiphilic polymer coated CdSe/ZnS QD's were separately loaded in poly(NIPAM) hydrogels with varying concentrations of QD's. As the spectral properties of QD's are dependent upon temperature and the local environment, embedding QD's in a thermoresponsive polymer will result in a change in the PL intensity and/or the position of the peak emission wavelength of the QD-thermoresponsive polymer nanocomposite hydrogel with temperature. A systematic study was carried out to probe the effects of temperature variation on the emission properties of the nanocomposite hydrogel samples. This work has a potential to serve as

a useful guideline in providing a comprehensive understanding of the feasibility of developing QD-thermoresponsive polymer nanocomposite hydrogel based optical temperature sensors.

CHAPTER III

EXPERIMENTAL

This chapter describes the materials and methods that were used in this study, the procedure for synthesis of CdSe/ZnS QD's in a MW reactor and the procedure for making QD's water soluble with an amphiphilic polymer coating followed by incorporating them in poly(NIPAM) hydogels.

3.1 Materials

Cadmium oxide (CdO, 99.99%, Alfa Aesar), tetradecylphosphonic acid (TDPA, 98%, Alfa Aesar), tri-*n*-octylphosphine oxide (TOPO, 99%, Aldrich), selenium (99 %, Aldrich), tri-n-octylphosphine (TOP, 99%, Aldrich), dimethylzinc (DMZ-1M in heptane, Aldrich), hexamethyldisilathiane (HMDS, Aldrich), polyethylenemine (PEI, 25 kD, Aldrich) were used as received. Anhydrous methanol and chloroform were purchased from Sigma-Aldrich.

The monomer *N*-isopropylacrylamide (NIPAM; 97%, Aldrich) was purified by recrystallization using hexane and dried under vacuum before use. The crosslinker *N*, *N*'-methylenebisacrylamide (BIS, Fluka), hydrophilic photoinitiator 1-[4-(2-hydroxyethoxy-phenyl]-2-hydroxy-2-methyl-1-propane-1-1 (Irgacure-2959, Aldrich). Deionized (DI) water was used in all experiments.

3.2 Methods

3.2.1 QD synthesis

Luminescent CdSe/ZnS core-shell QD's were synthesized in the laboratory by modifying a previously reported method by Peng et al. [11]. The synthesis reaction was performed in a single mode CEM Discover system operating at 300 W, 2.45 GHz. CdO (0.0514 g, 0.4 mmol) along with TDPA (0.0566 g, 0.2 mmol) and TOPO (3.7768, 9 mmol) were heated with continuous stirring in a 125 ml glass flask. The mixture was heated to approximately 300 °C under argon (Ar) flow (approx. 1 ml/sec) for 25 min to reduce CdO to form Cd^{2+}. TDPA acts as a stabilizer and helps in binding of Cd^{2+} to the coordinating solvent, TOPO.

TOP:Se stock solution was prepared beforehand in a small 25 ml round bottom flask by dissolving Se powder (0.0411 g, 0.5 mmol) in TOP (2.4 ml). The sealed flask was heated to 70 °C with continuous stirring on a hot plate equipped with a magnetic stirrer. Periodic Ar purging of the TOP:Se solution prevented the oxidation of TOP.

At approx. 265 °C TOP:Se was swiftly injected to start the nucleation process. The reaction time was varied between 1 to 4 min depending upon the desired emission wavelength of the QD's. The nucleation temperature, reaction time and MW power were dynamically controlled in real time through computer software interfaced with the MW reactor.

To improve the quantum yield and to protect the bare CdSe cores, a zinc sulfide (ZnS) shell was grown on them. To form the outer inorganic shell, the reaction temperature was reduced to approx. 180 °C and ZnS precursors made from DMZ (1.6

ml), HMDS (0.42 ml) and TOP (6.3 ml) was added drop wise (approx. 3 ml/min) into the reaction vessel. Approx. 30 min of heating ensures the formation of about 2 monolayers of ZnS shell around the cores. The core-shell QD's were then annealed at 100 °C for another 30 min. Finally the reaction was quenched using anhydrous methanol. The QD's samples were cleaned three times with methanol to remove excess unreacted precursors. The QD samples were then redispersed in chloroform or toluene until further use.

3.2.2 Amphiphilic polymer coating of QD's

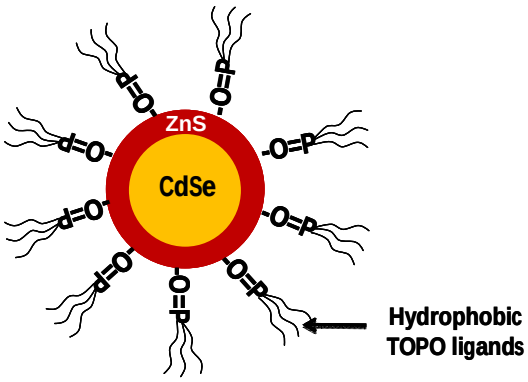

Figure 10. Schematic representation of TOPO capped QD's.

QD's synthesized in TOPO using the method described above were dispersed in a non-polar solvent e.g. chloroform or toluene for storage. QD's have a hydrophobic surface layer (Figure 10) and form sterically stabilized colloids in non-polar solvents and coagulate in polar solvents [36]. In order to incorporate these QD's in the thermoresponsive polymer hydrogels, it was necessary to perform a phase transfer of

QD's from chloroform to DI water. This was achieved by coating the QD's with an amphiphilic polymer, PEI [36].

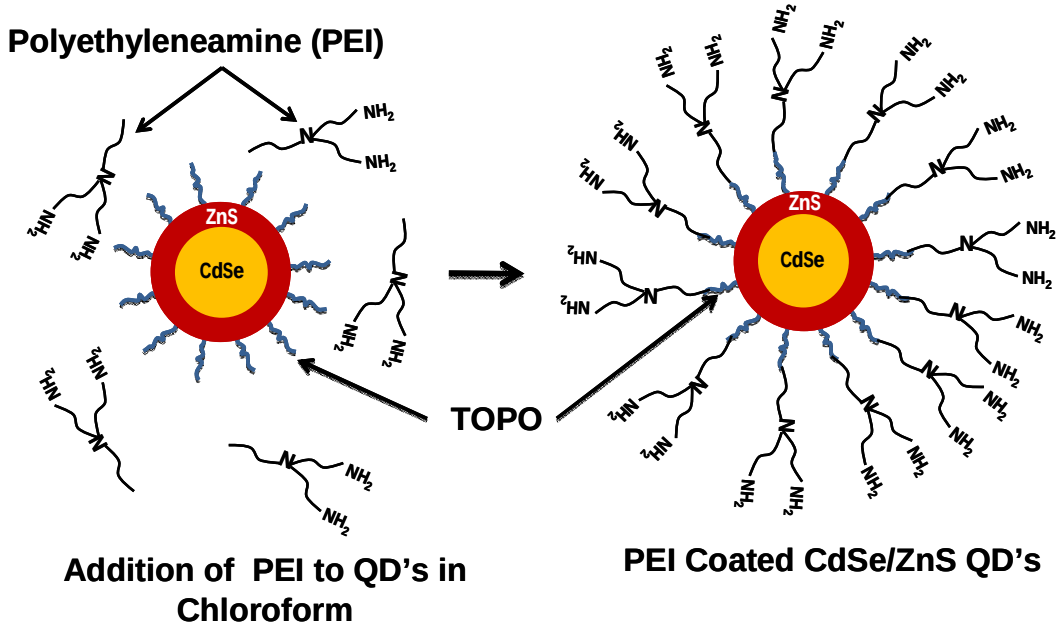

Figure 11. Schematic representation of PEI coating of CdSe/ZnS QD's.

The hydrophobic layer on the QD's was exchanged with PEI in chloroform (Figure 11). 1 mg of branched PEI was added to 10 ml of CdSe/ZnS QD's in chloroform inside a scintillation vial. This mixture was thoroughly vortexed until the PEI was dissolved in the solvent. The phase transfer was performed after 24 hours of adding PEI through direct extraction of the QD's from the chloroform with water. The solution was repeatedly centrifuged at 13400 RPM to yield an optically clear supernatant of CdSe/ZnS/PEI QD's dispersed in water.

3.2.3 Polymerization of NIPAM

Poly(NIPAM) hydrogels were formed by the process of photopolymerization [37]. 0.28 g (2.4 mmol) of NIPAM was dissolved in 1.5 ml water followed by addition of 0.01 g (64 μmol) of BIS and 0.01 g (44 μmol) of photoinitiator. The solution was purged with argon for 5 min with continuous stirring. Photopolymerization was carried out using a long range UV lamp (365 nm, 16 W) for 10 min inside a poly(methyl methacrylate) (PMMA) cuvette. The temperature of the system was maintained below the LCST at approx. 4 °C using an ice bath.

3.2.4 Incorporation of QD's in poly(NIPAM) hydrogels

As a novel approach, PEI coated QD's were incorporated in poly(NIPAM) hydrogels by carrying out *in situ* photopolymerization of the monomer and QD's in water in the presence of cross linker and photoinitiator. To best of my knowledge there have been no previous reports of incorporation of PEI coated CdSe/ZnS QD's in poly(NIPAM) hydrogels. Photopolymerization was carried out inside 1.5 ml PMMA disposable cuvettes (Plastibrand, Germany) having dimensions 12.5 x 12.5 x 45 mm.

3.3 Characterization

Absorption spectra were recorded on a Hitachi U-4100 UV-VIS-NIR spectrophotometer. Temperature dependent PL spectra were recorded on a PTI – 'Quanta Master' spectrofluorometer equipped with a temperature controlled cuvette holder (Figure 12).

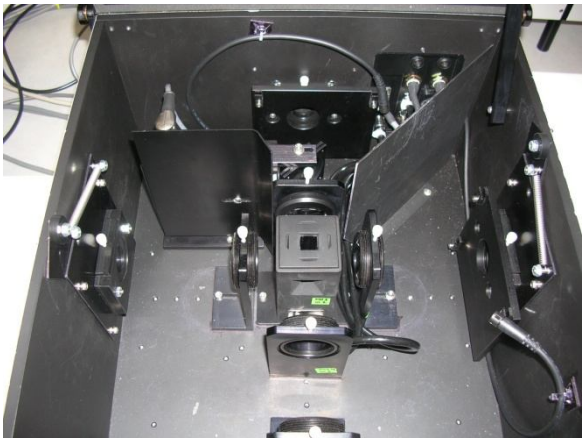

Figure 12. PTI ‘Quanta Master’ spectrofluorometer with temperature controlled cuvette holder.

Transmission electron microscopy images were recorded on JEOL 1200 EX transmission electron microscope. Standard TEM copper grids (3.05 mm diameter, Electron Microscopy Sciences, USA) were first coated with formwar (polyvinyl formal) followed by a coating of carbon using a carbon coater. The formwar film on the grid was dissolved using chloroform, leaving behind grids coated with a thin film of carbon. Approx. 3 μL of less than 0.1 μM concentration QD sample in chloroform was placed on the carbon coated grids for 30 sec. Excess sample was blotted dry with the help of a blotting paper placed perpendicular to the grid.

CHAPTER IV

RESULTS

This chapter summarizes all the results obtained during this project. Detailed procedures described in the previous chapter were followed for synthesis core-shell QD's followed by their incorporation in poly(NIPAM) hydrogels. Structural characterizations of the QD samples were performed using TEM. Optical characterizations were performed to investigate the temperature dependent emission properties of PEI coated QD's in water and QD/PEI/poly(NIPAM) hydrogels.

4.1 QD synthesis

Luminescent CdSe/ZnS QD's emitting at different wavelengths were synthesized using MW based synthesis system implemented as shown in Figure 6. Post synthesis, QD's were washed twice with methanol and were suspended in a non-polar solvent, e.g. chloroform, for storage. Figure 13 shows image of QD's of four different sizes (A, B, C and D) with peak emission ranging from 548 to 605 nm. Longer emission wavelengths correspond with the increasing size of the QD formed due to longer reaction times ranging from 1 to 4 min.

Figure 13. CdSe/ZnS QD's in chloroform as seen in ambient light (L) and under UV light (R).

4.2 Optical and structural characterization

4.2.1 TOPO capped QD's

Figure 14 shows the normalized emission spectra of QD samples A, B, C and D suspended in chloroform in the emission scan range from 500 to 700 nm with 465 nm excitation. The integration time was kept constant at 1 sec for all the scans. Small amount of inherent inhomogeneity in the size distribution of the samples results in the broadening of the emission spectra commonly referred to as the 'inhomogeneous broadening'. This broadening can be estimated by calculating the FWHM (full width at half maximum) of the Gaussian emission spectra of the samples. The FWHM of the samples were in the range of 40 to 50 nm.

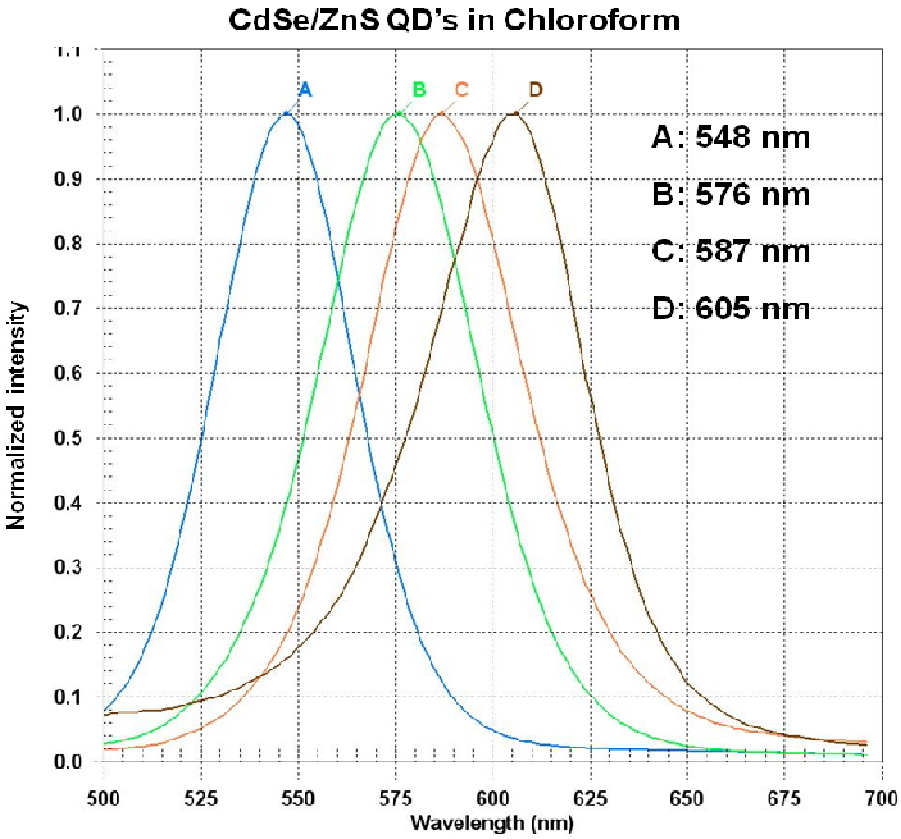

Figure 14. Normalized emission spectra of CdSe/ZnS QD's in chloroform.

Structural characterization of the QD samples was performed using TEM imaging. TEM grids for the four different QD samples were prepared by following the method discussed in the previous chapter. The grids were observed under JEOL 1200 EX transmission electron microscope operated at an acceleration voltage of 100 keV. TEM micrographs were recorded on Kodak 4489 films at a calibrated magnification of 70,200. The resolution of the system was calculated and found to be 2.85 A°/ pixel. Figure 15 and Figure 16 shows the TEM micrographs of QD samples A, B, C and D. In

order to determine the average particle size, the TEM micrograph films were scanned at 1270 DPI to digitize the image. The digitized images were then analyzed with the help of a GNU image manipulation program, GIMP Version 2.6.2. Using the built in measuring tool function the size of the particles in number of pixels was measured. This information along with the resolution of the system gave an estimate of the actual size of the particle. 10's of such nanoparticles in the image were measured and averaged to determine the average size of the QD's in the given sample. Basic statistical analysis was performed on the measured QD sizes to determine the standard deviation for each of the four QD samples. The sizes of the QD samples were also estimated using an empirical fitting function (1) used for determining the sizes of CdSe cores [38]. Approx. 1 nm radial thickness for the ZnS shell of about 2 monolayers was assumed for calculating the theoretical sizes of the synthesized CdSe/ZnS core-shell QD's. In the following equation, D (nm) is the calculated size of the CdSe core and λ (nm) is the wavelength of the first excitonic absorption peak of the corresponding QD sample.

$$\text{CdSe: } D = (1.6122 \times 10^{-9})\lambda^4 - (2.6575 \times 10^{-6})\lambda^3 + (1.6242 \times 10^{-3})\lambda^2 - (0.4277)\lambda + (41.57) \quad (1)$$

Peak emission wavelengths and size approximation for the four QD samples A, B, C and D are summarized in Table 1.

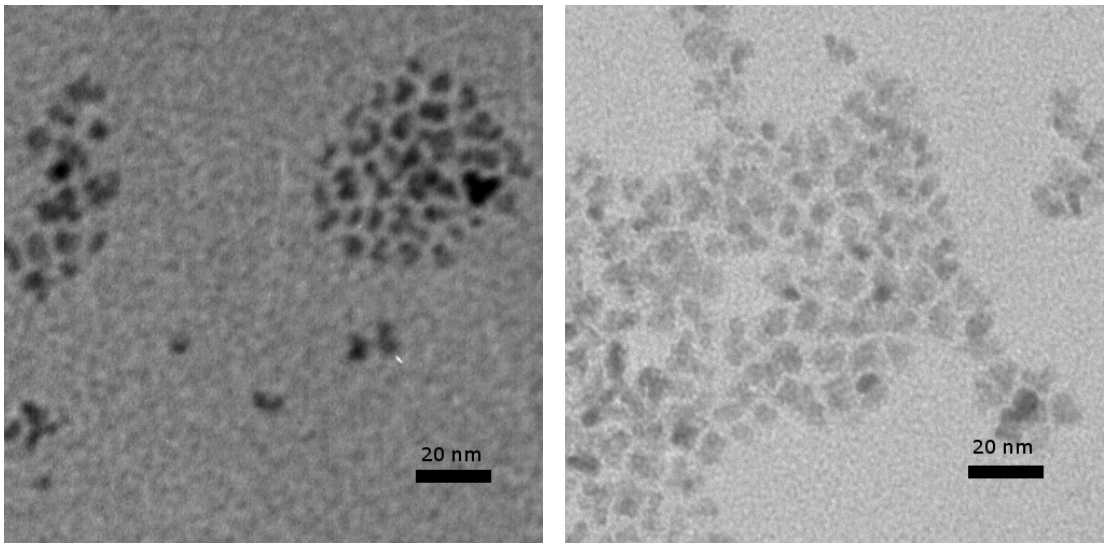

Figure 15. TEM micrograph of QD sample A (L) and QD sample B (R).

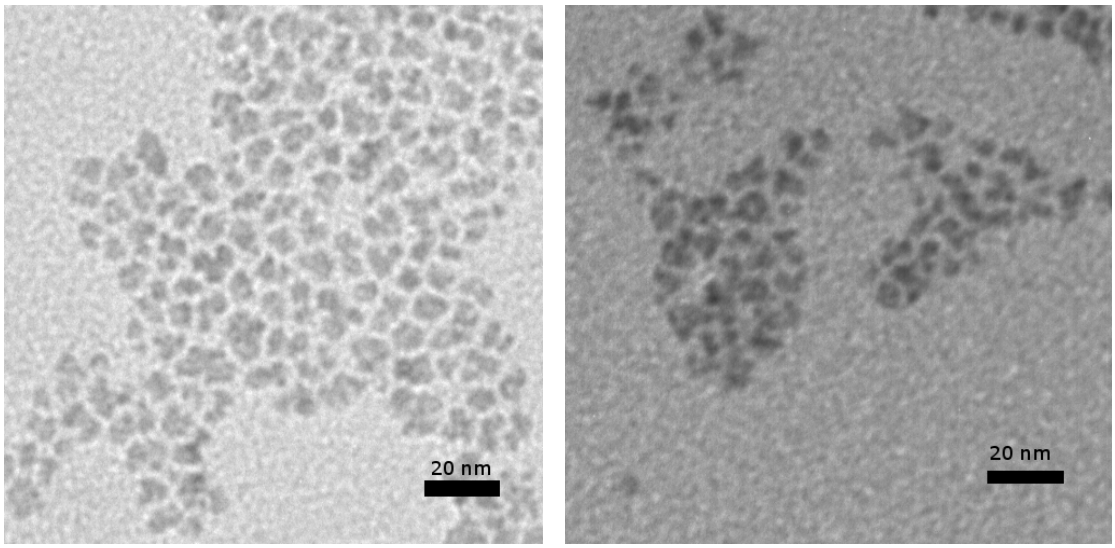

Figure 16. TEM micrograph of QD sample C (L) and QD sample D (R).

Table 1. Peak emission wavelengths and size approximation of QD sample A, B, C and D.

QD sample	Peak Emission (nm)	Estimated size (nm)	Measured size (nm)
Sample A	548	4.79	3.8 ± 0.57
Sample B	576	5.36	4.3 ± 0.68
Sample C	587	5.66	4.6 ± 0.6
Sample D	605	6.29	5.5 ± 0.7

4.2.2 PEI coated QD's

To make the QD's water soluble, TOPO capped QD's were coated with PEI in chloroform. Figure 17 shows the image of two of the above synthesized CdSe/ZnS samples A and B after coating with PEI followed by suspension in DI water. The PEI coated QD samples are denoted by A' and B' respectively. Figure 18 shows the emission spectra of QD samples before and after PEI coating. On comparing the emission spectra of QD's in chloroform and PEI coated QD's in water, it was observed that after PEI coating there was a red shift of 4 nm in peak emission position of both the samples A' and B'. This observation is consistent with reports of red shift in QD emission due to coating with an amphiphilic copolymer [39]. The FWHM of the emission spectra before and after PEI coating remained the same.

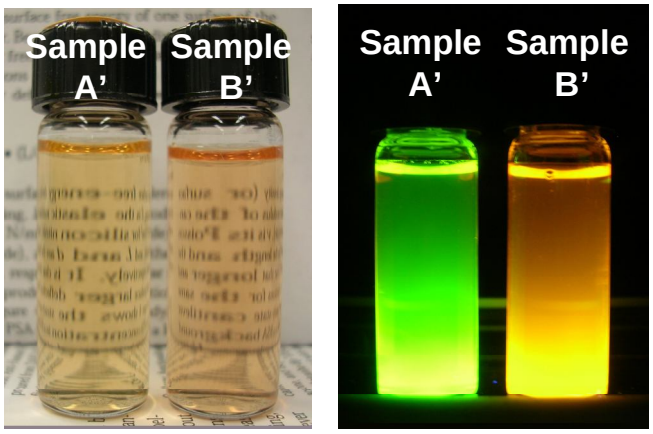

Figure 17. QD/PEI in DI water as seen in ambient light (L) and under UV light (R).

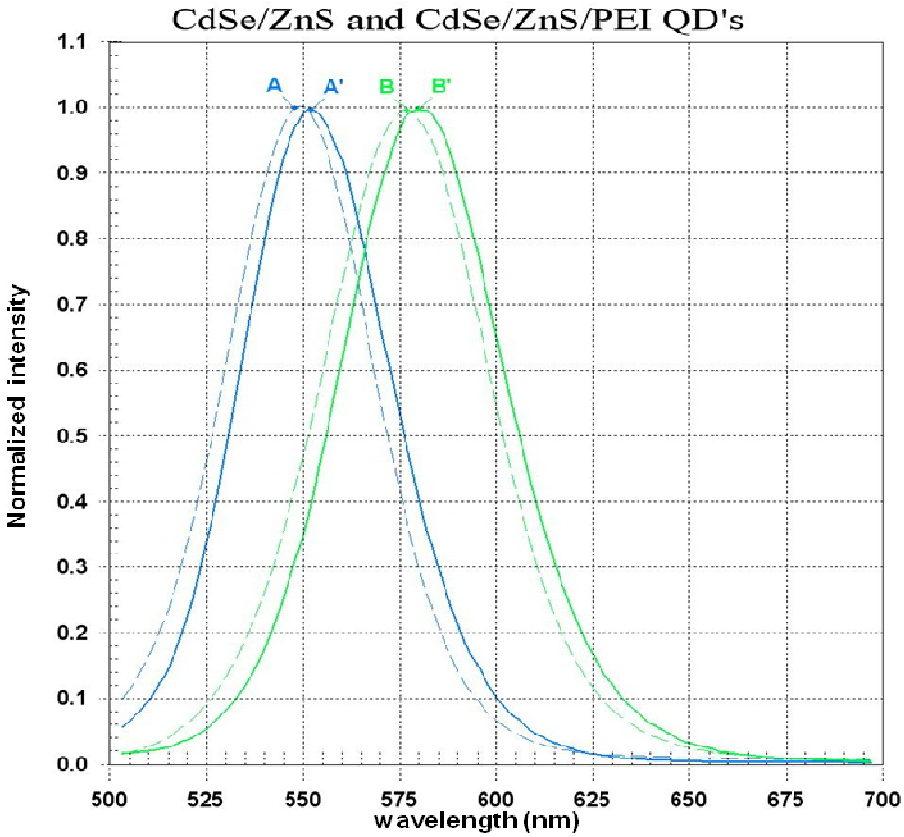

Figure 18. Normalized emission spectra of QD's (dotted) in chloroform and QD/PEI (solid) in DI water. Sample A (peak at 548 nm), Sample B (peak at 576 nm), Sample A' (peak at 552 nm) and B' (peak at 580 nm).

4.3 Poly(NIPAM) hydrogels

Poly(NIPAM) hydrogles were prepared by polymerization of the monomer, crosslinker in the presence of a photosensitive hydrophilic polymerization initiator in DI water. Figure 19 shows an image of plain poly(NIPAM) hydrogel casted inside a glass vial by photopolymerization method described in previous chapter. Figure 20 shows the thermoresponsive behavior of poly(NIAPM) hydrogel. At temperatures across the LCST reversible phase transformation occurs inside the polymer matrix.

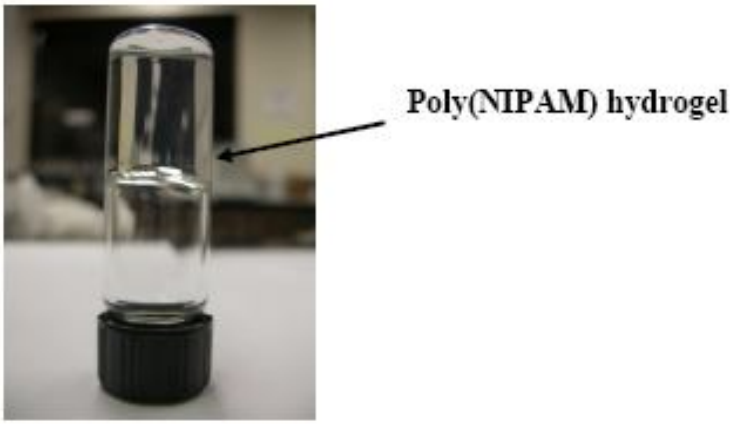

Figure 19. Poly(NIPAM) hydrogel casted inside a glass vial.

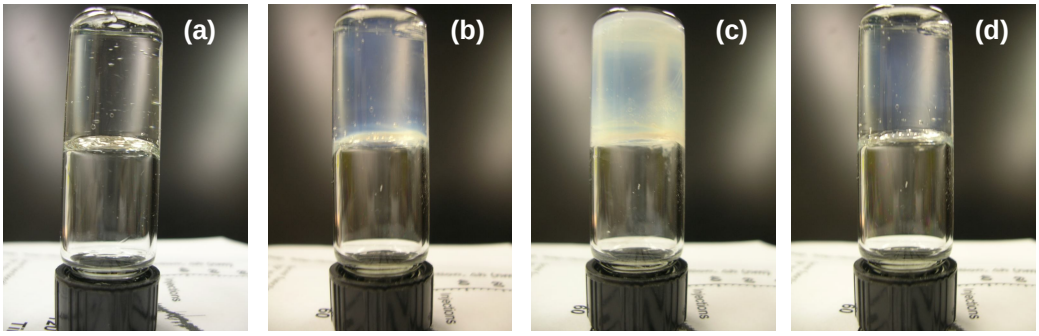

Figure 20. Thermoresponsive behavior of poly(NIPAM) hydrogel.
(a) at room temperature, (b) at temperature at which phase transition just occurs, (c) at temperature greater than LCST and (d) on returning back to room temperature.

4.4 QD/PEI/poly(NIPAM) nanocomposite hydrogels

PEI coated QD's suspended in DI water were incorporated inside poly(NIPAM) hydrogels by directly carrying out the photopolymerization of the NIPAM monomer in the solvent (QD/PEI in DI water) in presence of crosslinker and polymerization initiator. Figure 21 shows images of plain poly(NIPAM) and poly(NIAPM) embedded with QD's.

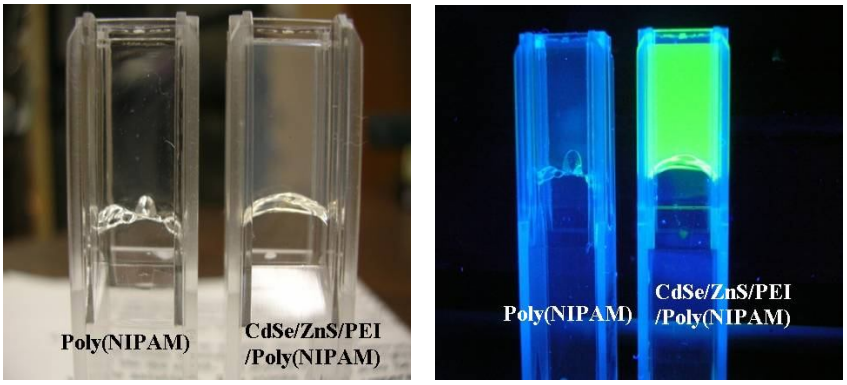

Figure 21. Poly(NIPAM) and QD/PEI/poly(NIPAM) hydrogels as seen in ambient light (L) and under UV light (R).

The final aim of this experimental work was to separately load PEI coated QD's with increasing concentration inside the poly(NIPAM) and study the effects of temperature variation on the PL spectra of the nanocomposite hydrogels. A high concentrated sample of PEI coated QD's dots (peak emission at RT ~ 576 nm and FWHM 42 nm) was prepared. Calculated dilution of this sample was carried out to obtain samples with three different concentrations. Low concentration being ~ 0.28 μM, medium ~ 1.43 μM and high ~ 2.86 μM. The concentration of QD's in the solution was estimated using a method describe elsewhere [38]. Briefly, first absorption peak (A_m) was obtained from the absorption spectra; FWHM of the PL spectra was obtained from the emission spectrum. Calibrated absorbance (A) was calculated as $A = (A_m*FWHM)/25$. Finally, concentration (C) in mol/L was calculated as $C = A/\varepsilon$ where, ε is the extinction coefficient per mole of QD's expressed in $cm^{-1}mol^{-1}$. Figure 22 shows PEI coated QD's at low, medium and high concentration. Approx. 1.5 ml of each of the three QD samples were loaded separately in poly(NIPAM) hydrogels. The photopolymerization process was carried out inside semi micro PMMA cuvettes as shown in Figure 23. The PL spectra for each of the nanocomposite hydrogel samples were recorded in the temperature range from 29 to 37 °C at 2 °C increments. Emission scan range was 470 to 700 nm at fixed excitation of 450 nm. The emission and excitation slits were set at 1.5 nm and the integration time was kept constant at 0.1 sec. The emission spectra were collected after a brief interval of 3.5 min between each temperature change to ensure thermal equilibrium between the set temperature and the actual temperature of the hydrogel. To delineate the effects of phase transformation due

to poly(NIPAM) polymer on the emission properties of embedded QD's as a control the emission spectra of each of the QD/PEI samples suspended in water were also collected in the temperature range from 29 to 37 °C at 2 °C increments at same instruments settings. Figures 24 to 26 show the emission spectra of the PEI coated QD's suspended in water at low, medium and high concentrations respectively.

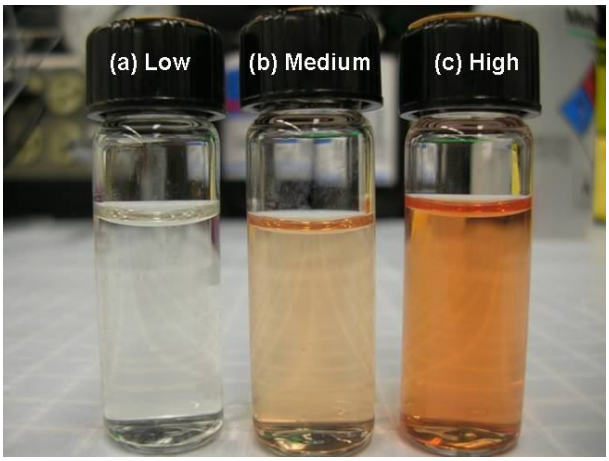

Figure 22. QD/PEI in DI water at three different concentrations. (a) low concentration: ~ 0.28 µM, (b) medium concentration: ~1.28 µM and (c) high concentration: ~2.86 µM.

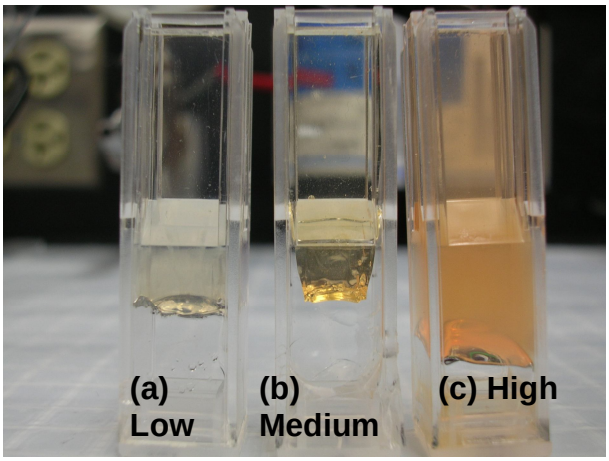

Figure 23. QD/PEI/poly(NIPAM) hydrogels at three different concentrations. (a) low concentration sample, (b) medium concentration sample and (c) high concentration sample.

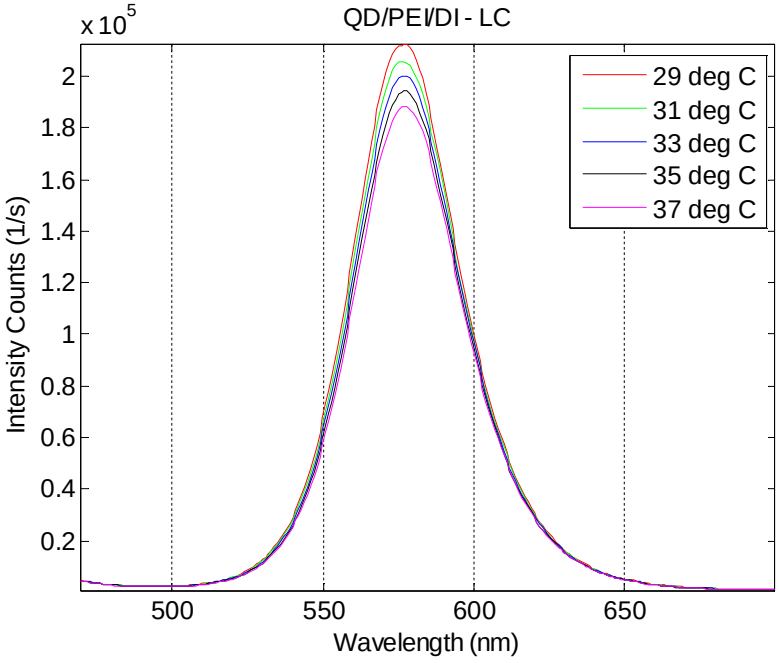

Figure 24. Temperature dependent emission spectra of QD/PEI in DI water - low concentration sample.

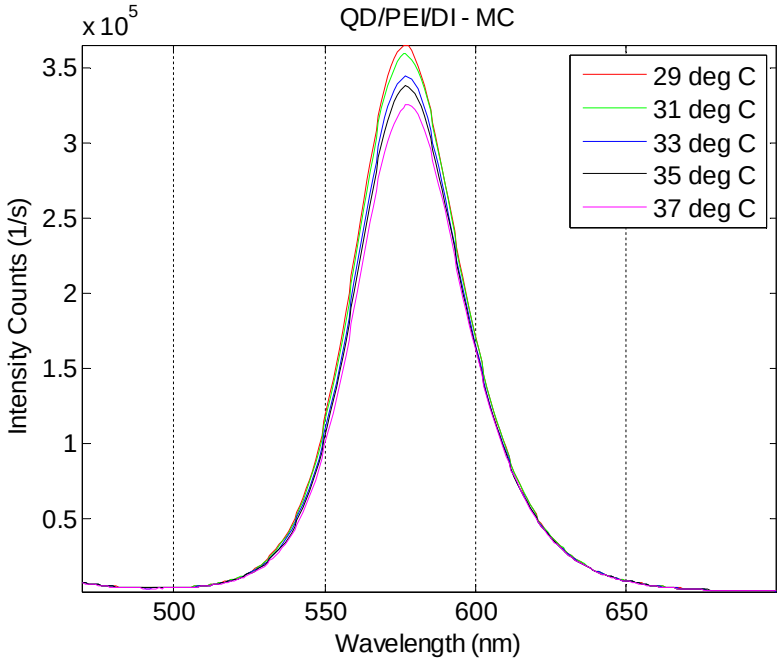

Figure 25. Temperature dependent emission spectra of QD/PEI in DI water - medium concentration sample.

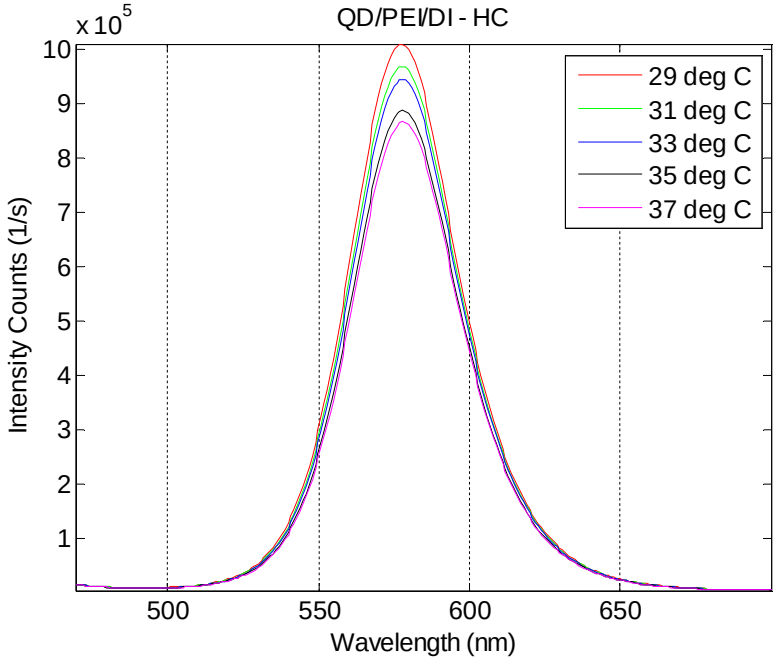

Figure 26. Temperature dependent emission spectra of QD/PEI in DI water - high concentration sample.

It can been observed that on increasing the temperature from 29 to 37 °C the emission intensity linearly decreases without any change in the position of the peak emission wavelength for each of the three QD/PEI samples. Figure 27 shows the emission spectra of plain poly(NIPAM) hydrogel with respect to temperature. I speculate that the characteristics peak in the emission spectra arise due to the scattering of excitation light and inherent nature of the monochromator. The information in this spectra will be used later for background subtraction from the raw temperature dependent emission spectra of QD/PEI/poly(NIPAM) hydrogel samples.

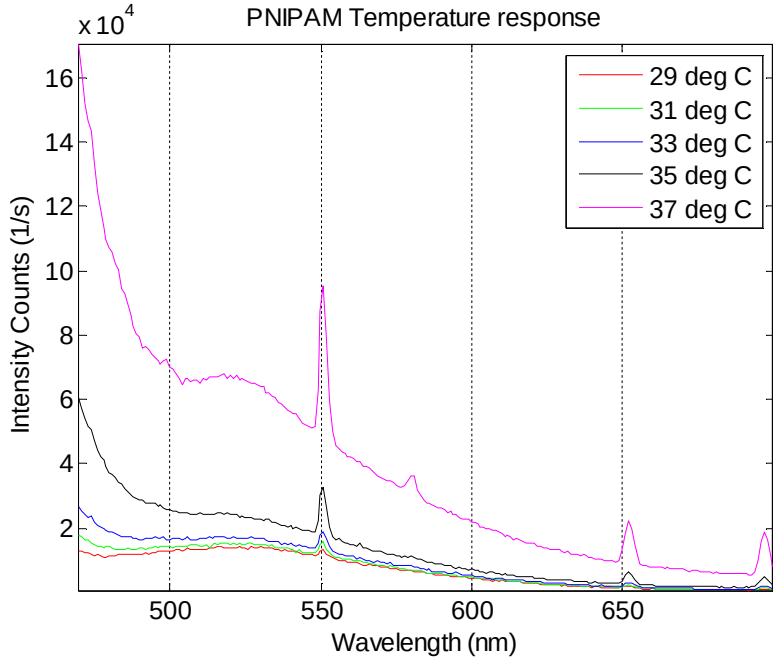

Figure 27. Temperature dependent emission spectra of plain poly(NIPAM) hydrogel.

Figures 28 to 30 show the raw temperature dependent emission spectra of QD/PEI/poly(NIPAM) hydrogel samples at low, medium and high concentration respectively. It can be seen that there is a large of background contribution due to poly(NIPAM) and it is more apparent for low and medium concentration sample where the overall luminescence is lower. To accurately estimate the effects of temperature variation on the emissions properties of the QD's incorporated inside poly(NIPAM) hydrogel it was necessary to eliminate the background contribution due to poly(NIPAM). Detailed discussion of the experimental results and poly(NIPAM) background subtraction technique is provided in the next chapter.

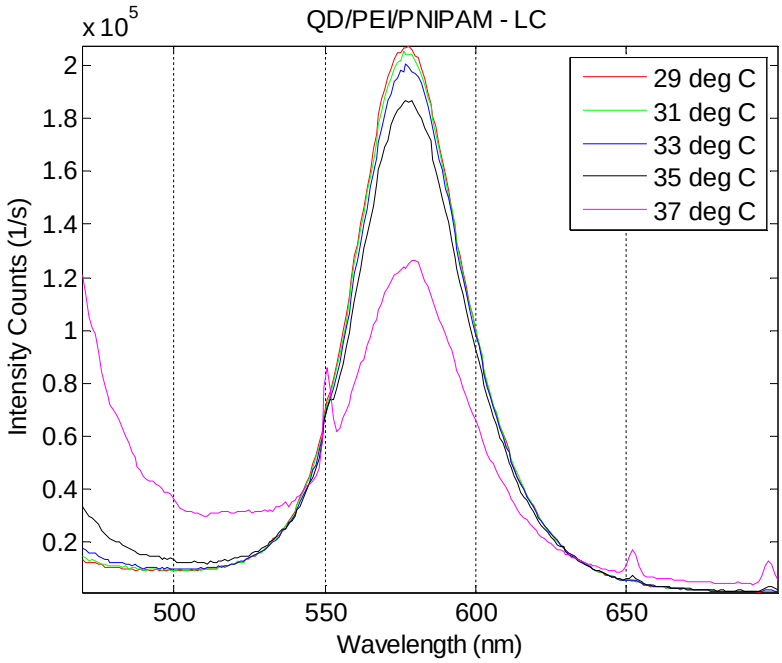

Figure 28. Temperature dependent emission spectra of QD/PEI/poly(NIPAM) hydrogel - low concentration sample.

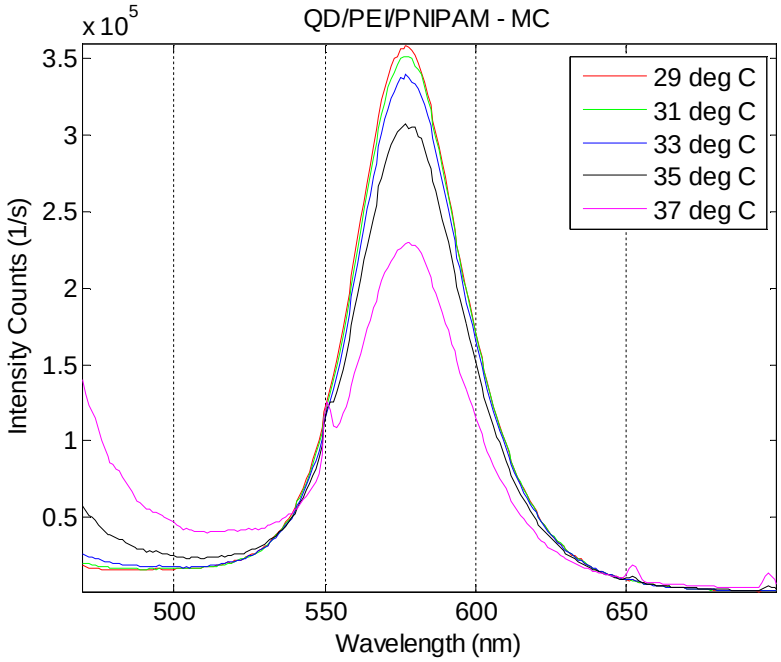

Figure 29. Temperature dependent emission spectra of QD/PEI/poly(NIPAM) hydrogel - medium concentration sample.

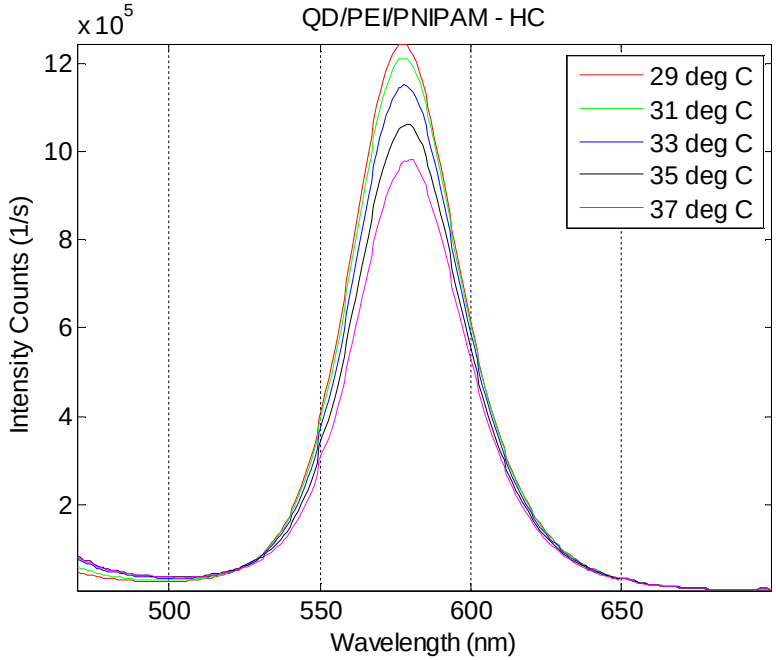

Figure 30. Temperature dependent emission spectra of QD/PEI/poly(NIPAM) hydrogel - high concentration sample.

CHAPTER V

DISCUSSION

The experiments reported in this work present a novel method for the preparation of QD-thermoresponsive polymer nanocomposite hydrogels. CdSe/ZnS QD's were successfully synthesized in a MW reactor by following one pot synthesis procedure. The MW system allowed precise control of the reaction parameters such as nucleation temperature and reaction time which in turn controlled the emission wavelength (size) of the QD's. TEM characterization of the samples showed that the synthesized QD's were monodisperse and they did not aggregate in the solvent. With the implementation of MW based system reproducibility of QD synthesis results was possible as the reaction parameters were now automatically controlled with the help a computer software program interfaced with the MW reactor thus, minimizing errors due to imprecise temperature control and timing variation as compared to manually employed procedures in a metal bath reactor.

PEI coating of the QD's provided us with a straight forward method for performing the phase transfer of QD's from chloroform to water. Post coating with PEI the QD's formed highly stable colloids in water and did not redisperse back in non-polar solvents. PEI coated QD's presented good compatibility with poly(NIPAM) hydrogels following the method of photopolymerization. The QD/PEI/poly(NIPAM) hydrogels maintained their PL intensity for several hours followed by gradual decrease in the PL intensity possibly due to photooxidation effects [36]. Recrystallization of the NIPAM

monomer by hexane, prior to use helped remove some of the impurities which in other case had drastically affected the PL intensity of the embedded QD's.

Raw temperature dependent emission spectra of QD/PEI/poly(NIPAM) hydrogels shows the presence of characteristic peaks similar to that seen for plain poly(NIPAM) hydrogel. These peaks were more prominent at temperatures higher than the LCST (35 and 37 °C). At temperatures above the LCST poly(NIPAM) undergoes a phase transition resulting in collapse of the hydrogel and presents a nonlinear behavior with respect to temperature as shown in Figure 27. In order to estimate the change in the position of peak emission wavelength for the QD/PEI/poly(NIPAM) samples with temperature, it was necessary to remove the background contribution due to poly(NIPAM). A straight forward method to remove this background was to perform the direct spectral subtraction of the emission data of plain poly(NIPAM) hydrogel from the emission data of QD/PEI/poly(NIPAM) hydrogels at a given temperature. Figures 31 to 33 show the background free emission spectra of QD/PEI/poly(NIPAM) samples at low, medium and high concentration respectively obtained following the method of direct spectral subtraction. Direct spectral subtraction of the emission data for temperatures lower than LCST (29, 31 and 33 ºC) eliminated the poly(NIPAM) background effects to some extent but for temperatures higher than the LCST (35 and 37 ºC) it resulted in negative y-axis values particularly for wavelengths lower than 540 nm. Due to the nonlinear behavior of poly(NIPAM) emission a slight variation at a given temperature possibly due to temperature controller inconsistency resulted in large variations in the overall emission spectra particularly at lower wavelengths in the range from 470 to 540

nm. Hence, direct spectral subtraction of the emission data was not a feasible way to eliminate the poly(NIPAM) background.

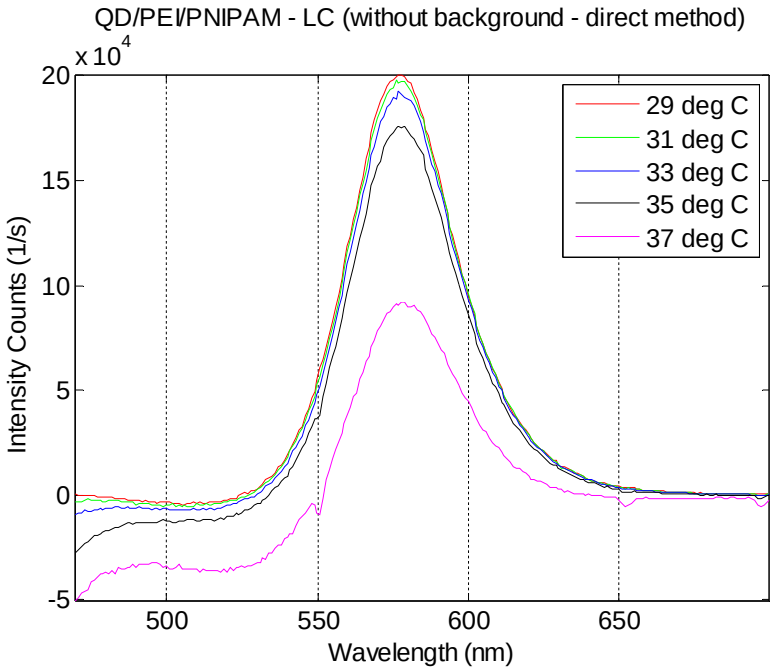

Figure 31. Temperature dependent emission spectra of QD/PEI/poly(NIPAM) hydrogel after background subtraction via direct method - low concentration sample.

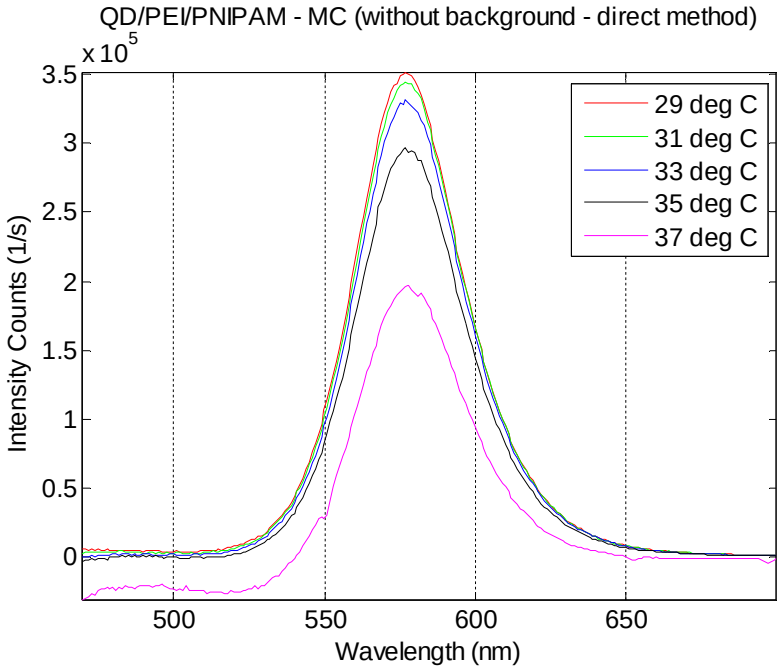

Figure 32. Temperature dependent emission spectra of QD/PEI/poly(NIPAM) hydrogel after background subtraction via direct method - medium concentration sample.

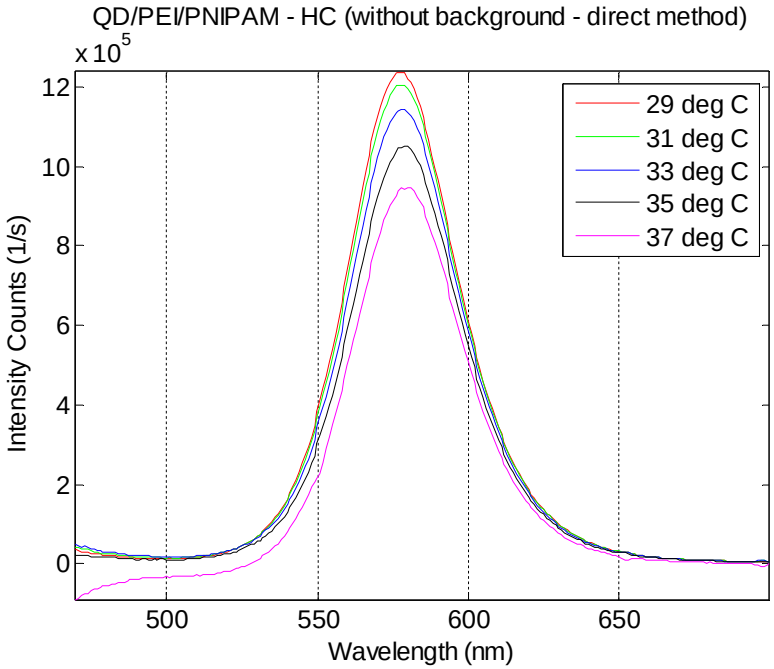

Figure 33. Temperature dependent emission spectra of QD/PEI/poly(NIPAM) hydrogel after background subtraction via direct method - high concentration sample.

An algorithm was developed in MATLAB that interpolated the temperature dependent emission spectra of the poly(NIPAM) hydrogel in the temperature range from 29 to 37 °C in steps of 0.1 °C at each wavelength in the emission scan range from 470 to 700 nm. 'Spline' interpolation function in MATLAB was used to interpolate the temperature dependent emission spectra for the plain poly(NIPAM) hydrogel at correct temperature. The obtained spectra was then superimposed on the QD/PEI/poly(NIPAM) temperature dependent emission spectra to obtain an estimate of a best fit to the spectra of QD/PEI/poly(NIPAM) and the corresponding interpolate (corrected) temperature value was recorded. In other words, the interpolated temperature value was selected such that the temperature response of the plain poly(NIPAM) hydrogel matched as closely as possible to that of the QD/PEI/poly(NIPAM) hydrogel at that particular temperature in the lower wavelength range from 470 to 540 nm and higher than 640 nm. This interpolated poly(NIPAM) emission spectra was then subtracted from the original QD/PEI/poly(NIPAM) emission spectra to remove the poly(NIPAM) background. For example, Figure 34 shows the emission spectra of QD/PEI/poly(NIPAM) medium concentration sample at 37 ºC before and after background subtraction via interpolation method. It was observed that the emission spectra of poly(NIPAM) when interpolated at 36.3 °C in this case, completely removes the background from the raw QD/PEI/poly(NIPAM) emission spectra. A Savitzky–Golay smoothing filter algorithm was applied to this background free emission data to reduce noise and estimate the peak emission wavelength at that temperature. Savitzky–Golay smoothing filter is often used with spectroscopic data and it performs better than averaging filters in removing noise

without significantly compromising the features of the distribution such as relative maxima, minima and line width. A constant smoothing window of 7 nm was used as it was significantly smaller than the spectral width of the emission spectrum having FWTM (full width at tenth maximum) approx. 89 nm. Similar data processing operations were performed for the low, medium and high concentration QD/PEI/poly(NIPAM) samples at 29, 31, 33, 35 and 37 ºC. Figure 35 to 37 show the final background free temperature dependent emission spectra of QD/PEI/poly(NIPAM) samples at low, medium and high concentration respectively.

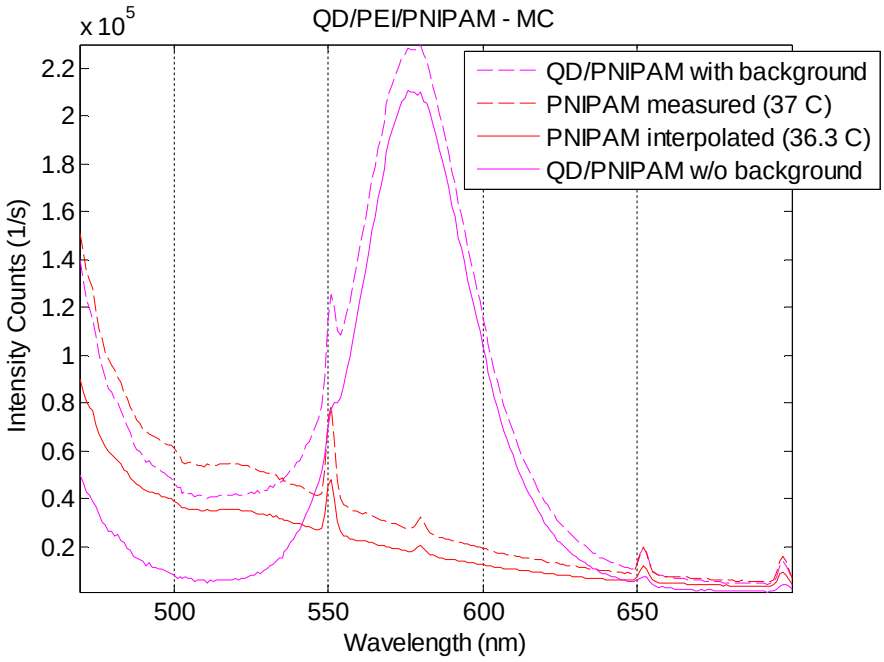

Figure 34. Emission spectra of QD/PEI/poly(NIPAM) - medium concentration sample at 37 ºC. Raw QD/PEI/poly(NIPAM) emission spectrum (blue dotted), QD/PEI/poly(NIPAM) emission spectrum after background subtraction (blue solid), poly(NIPAM) emission at measured temperature (red dotted) and poly(NIPAM) emission spectrum at interpolated temperature (red solid).

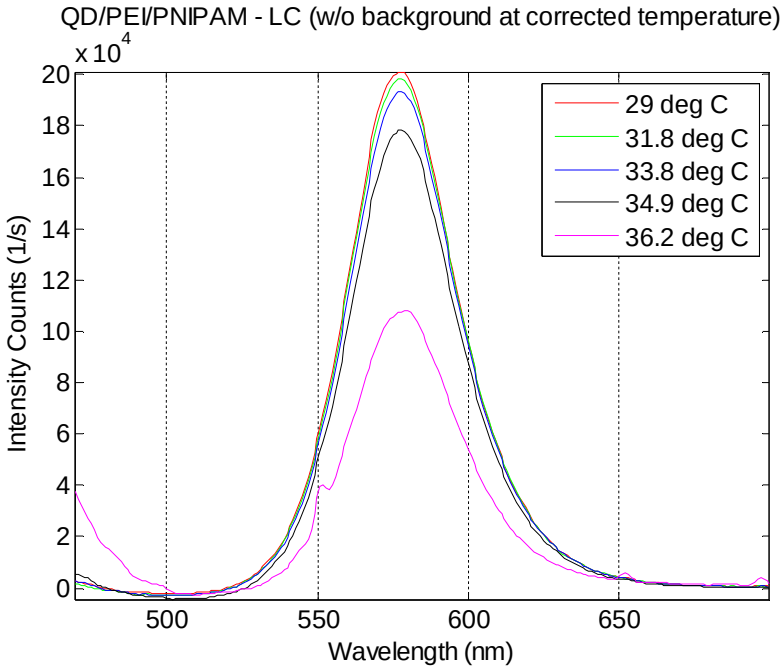

Figure 35. Temperature dependent emission spectra of QD/PEI/poly(NIPAM) hydrogel after background subtraction via interpolation method - low concentration sample.

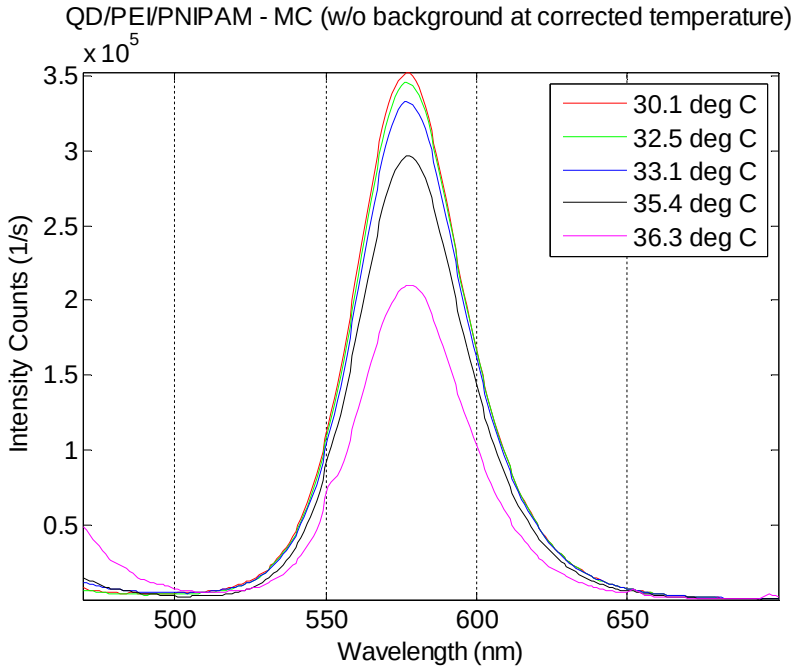

Figure 36. Temperature dependent emission spectra of QD/poly(NIPAM) hydrogel after background subtraction via interpolation method - medium concentration sample.

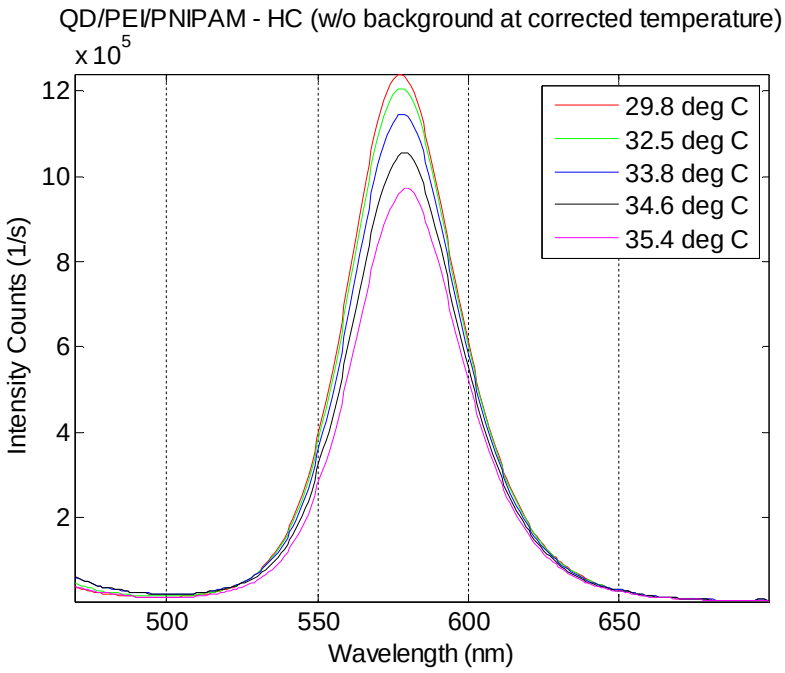

Figure 37. Temperature dependent emission spectra of QD/PEI/poly(NIPAM) hydrogel after background subtraction via interpolation method - high concentration sample.

In order to validate the results, a second set of QD/PEI/poly(NIPAM) samples (peak emission at RT ~ 577 nm and FWHM 42 nm) at low, medium and high concentration was prepared. The concentration of PEI coated QD's in these samples were within ± 25% of the previous batch and were estimated to be; ~ 0.21 µM (low concentration), ~ 1.28 µM (medium concentration) and ~ 3.06 µM (high concentration). The temperature dependent emission spectra of these samples were recorded in the temperature range from 29 to 37 °C at 2 °C increments. The emission scan range was 470 to 700 nm at fixed excitation of 450 nm. Following the procedure for poly(NIPAM) background subtraction via interpolation method, the peak emission wavelength and the corresponding corrected temperature value for each of the samples were recorded.

Figures 38 to 40 show the peak emission wavelength shift vs. corrected temperature for each of the QD/PEI/poly(NIPAM) samples at low, medium and high concentrations respectively. The temperature range represents the error between the thermocouple and the actual corrected temperature of the hydrogel samples obtained by interpolation.

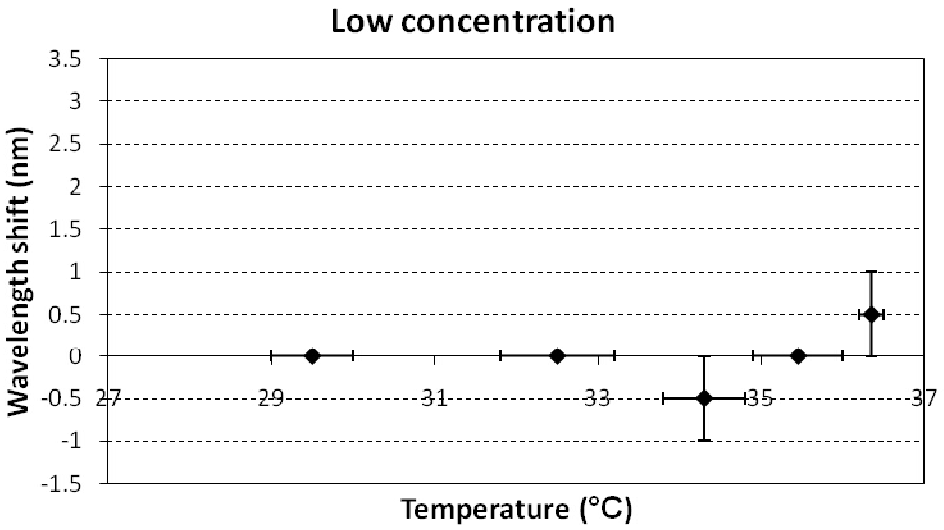

Figure 38. Peak emission wavelength shift vs. temperature for QD/PEI/poly(NIPAM) low concentration sample.

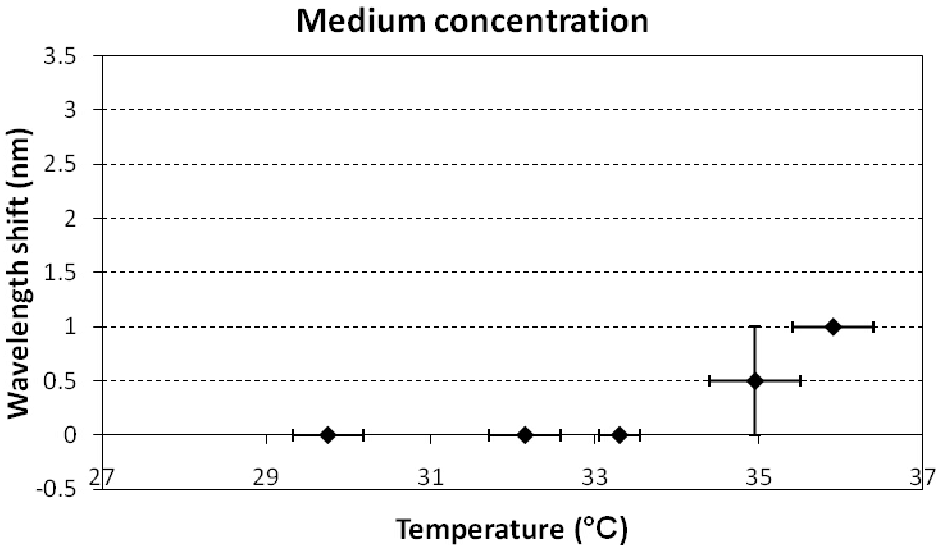

Figure 39. Peak emission wavelength shift vs. temperature for QD/PEI/poly(NIPAM) medium concentration sample.

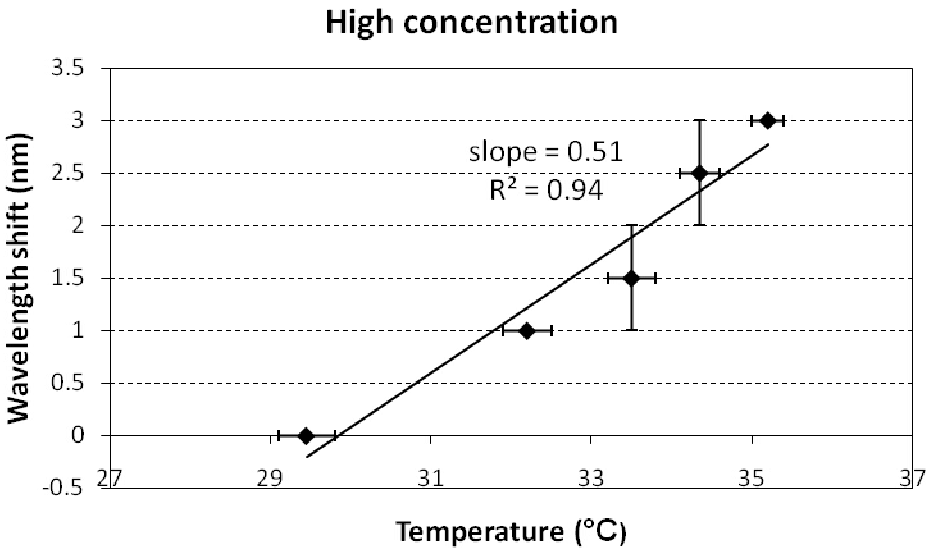

Figure 40. Peak emission wavelength shift vs. temperature for QD/PEI/poly(NIPAM) high concentration sample.

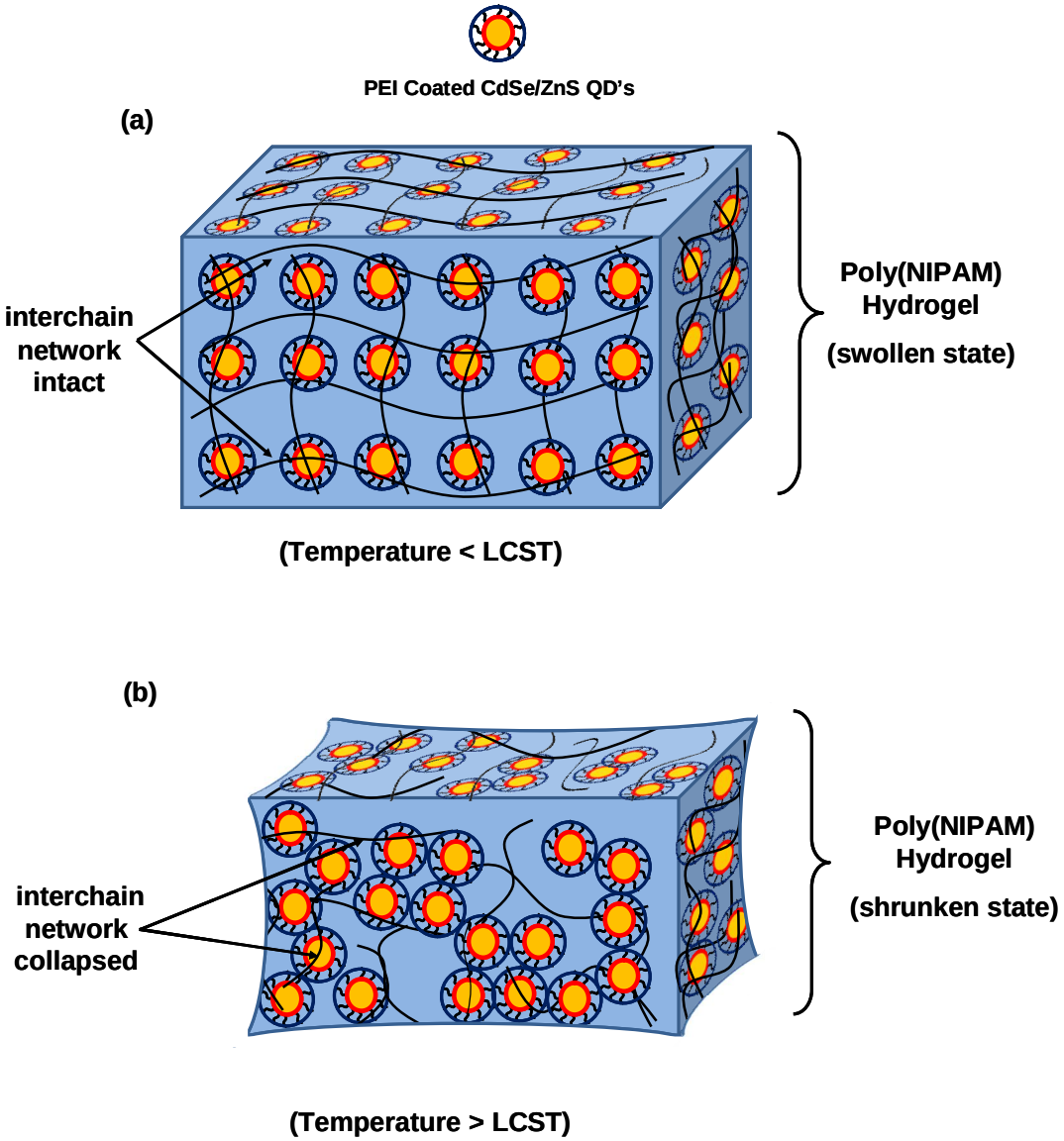

Figure 41. Schematic representation of QD's incorporated inside poly(NIPAM) hydrogel. (a) at temperature < LCST (swollen state) and (b) at temperature > LCST (shrunken state).

Figure 41 shows the schematic representation of thermoresponsive behavior of PEI coated QD's inside poly(NIAPM) hydrogel. At temperatures lower that the LCST the interchange network remains intact and I assumed that the PEI coated QD's are distributed homogenously throughout the hydrogel, represented by Figure 41 (a). At temperatures higher that LCST the interchain network collapses causing the PEI coated QD's to become close-packed in the hydrogel [16], represented by Figure 41 (b). This phenomenon accompanied by the overall shrinking of the hydrogel resulted in increased interaction between PEI coated QD's. For low concentration samples there is no shift of peak emission wavelengths with temperature (Figure 38). For medium concentration samples there is red shift of the peak emission wavelength at temperatures near the phase transition temperature of the hydrogel (Figure 39). For the high concentration samples there is an increasing linear red shift of the peak emission wavelength with temperature in the range from 29 to 36 °C (Figure 40). A linear regression fit was plotted for the high concentration sample and the slope of the fit was calculated to be approx. 0.5 nm/°C. Similar linear red shift of the peak emission wavelength with temperature in the range from 25 to 41 °C and slope approx. 0.81 nm/°C was reported by Li and coworkers [16]. This shift in peak emission wavelength was found to be reversible with temperature. There was no change observed in the FWHM of the emission spectra of the QD/PEI/poly(NIPAM) samples in the given temperature range i.e. the FWHM remained constant at 42 nm and it was independent of temperature. Hence, it can be deduced that there is a definite relation between the concentration of the QD's that are incorporated inside the hydrogel and their temperature dependent peak emission wavelength.

I have reduced the possibility of non-radiative energy transfer between individual dots by coating the QD's with an amphiphilic polymer, PEI. Typically, the distance over which Förster resonance energy transfer (FRET) occurs is in the range of 1 to 10 nm [40]. Bawendi and coworkers have demonstrated efficient resonance energy transfer between closed packed CdSe QD's with an inter dot spacing of approximately 1.1 nm. They calculated the critical radius for energy transfer, $R_0 = 4.7$ nm [41]. FRET efficiency varies as a function of the distance between the QD's. In my case, high molecular weight (25 kD) PEI coating of the QD's resulted in an average hydrodynamic diameter of 17.5 ± 2.5 nm [36]. Thus, the average distance between any two PEI coated QD's was greater than the Förster distance over which the energy transfer can occur efficiently. With the concentration information available, I estimated the interdot spacing between PEI coated QD's incorporated inside the poly(NIPAM) hydrogel for homogeneously distributed QD's. I assumed a cubic lattice type of geometry with PEI coated QD's homogenously distributed throughout the hydrogel. Figure 42 shows the schematic representation of the cubic lattice with PEI coated QD's present at each of its vertices. The interdot distance 'r' was calculated using the known concentration (C) and volume (V) information. Table 2 summarizes the estimated interdot distance for the low, medium and high concentration QD/PEI/poly(NIPAM) samples.

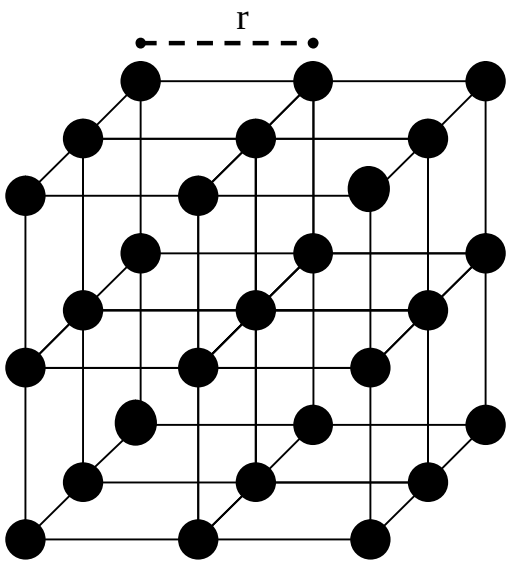

Figure 42. Schematic representation of the distribution of PEI coated QD's inside poly(NIPAM) hydrogel. 'r' is the interdot distance.

Table 2. Estimation of interdot spacing in QD/PEI/poly(NIPAM) samples.

Sample	**C (µmol/L)**	**V (L)**	**n = C x V (mol)**	**n x Avogadro constant***	**r (nm)**
Low	0.28	1.5e-3	4.2e-10	2.52e+14	181
Medium	1.28	1.5e-3	1.92e-9	1.15e+15	109
High	2.86	1.5e-3	4.29e-9	2.58e+15	83

* 6.023e+23

The estimated interdot spacing for the low, medium and high concentration samples were theoretically very large for energy transfer to occur efficiently. I speculate that the possible reason for the increasing red shift of the peak emission wavelengths for the medium and high concentration QD/PEI/poly(NIPAM) sample may have been due to interaction of PEI coated QD's resulting from the physical change in their surrounding environment due to collapse of the interchain network at temperatures greater than the LCST. PEI coated QD's are positively charged due to the presence of large number of free amine groups in PEI and reported to have a zeta potential of about +29 mV [42]. Loading PEI coated QD's at different concentrations was crucial as the experimental results suggest that this phenomenon depends upon the number of PEI coated QD's present inside the hydrogel. Increasing amount of red shift in the emission spectra was observed for the high concentration sample as compared to medium and low concentration sample of QD's under similar experimental conditions. Another possible reason for the red shift in the high concentration sample may be due to possible aggregation of the PEI coated QD's inside the hydrogel at temperatures higher than the LCST causing the emission spectra to shift red due to reabsorption of the excitation light. But, this would not have resulted in a linear red shift across the entire temperature range from 29 to 37 °C for my experiments and as reported by Li and coworkers in temperature range from 25 to 41 °C [16]. With my assumption that PEI coated QD's are distributed homogenously in the hydrogel matrix the possibility of energy transfer was reduced however, cannot be completely ruled out.

CHAPTER VI

CONCLUSION AND FUTURE WORK

This work demonstrated the successful implementation of an efficient method for synthesis of luminescent CdSe/ZnS core-shell QD's in a MW reactor. A MW based QD synthesis system proved to be much safer and time saving as compared to the previously used metal bath reactor system. It helped achieve better overall control of the reaction parameters with minimal human intervention. Optical and structural characterizations of the QD samples synthesized in the MW reactor were performed to estimate their peak emission wavelengths and their approximate size.

A novel method for the preparation of QD-thermoresponsive polymer nanocomposite hydrogel was presented. A straight forward method of coating the QD's with PEI for performing phase transfer from non-polar solvents to water was effectively utilized followed by the successful incorporation of PEI coated QD's in poly(NIPAM) hydrogel by method of photopolymerization. The temperature dependent emission properties of the QD/PEI/poly(NIPAM) samples showed a definite relation between change in the position of the peak emission wavelength and concentration of the incorporated PEI coated QD's. The possibility of energy transfer between individual QD's was reduced due to PEI coating and it was speculated that the changes in the physical environment i.e. shrinking and swelling behavior of the poly(NIPAM) hydrogel due to the temperature change across the LCST caused the spectral properties of the QD's change accordingly.

Future work will include conducting similar experiments to investigate the effects of various other QD-amphiphilic polymer coating sizes on the temperature dependent emission spectra for high concentration samples. Also, incorporation of QD's in a thermoresponsive polymer matrix enables us to form an optically active scaffold, fine tuning of this phenomenon would help to establish a correlation between the spectral changes and the corresponding temperature for potential optical temperature sensing applications. A possible limitation of such a system is the limited operational temperature range which is specifically across the LCST of the thermoresponsive polymer under consideration.

REFERENCES

[1] Alivisatos AP. Semiconductor clusters, nanocrystals, and quantum dots. Science 1996;271(5251):933-937.

[2] Ballou B, Lagerholm BC, Ernst LA, Bruchez MP, Waggoner AS. Noninvasive imaging of quantum dots in mice. Bioconjugate Chemistry 2004;15(1):79-86.

[3] Bruchez M Jr, Moronne M, Gin P, Weiss S, Alivisatos AP. Semiconductor nanocrystals as fluorescent biological labels. Science 1998;281(5385):2013-2016.

[4] Schlamp MC, Peng X, Alivisatos AP. Improved efficiencies in light emitting diodes made with CdSe(CdS) core/shell type nanocrystals and a semiconducting polymer. Journal of Applied Physics 1997;82:5837-5842.

[5] Chaudhary S, Ozkan M, Chan WCW. Trilayer hybrid polymer-quantum dot light-emitting diodes. Applied Physics Letters 2004;84:2925-2927.

[6] Huynh WU, Peng XG, Alivisatos AP. CdSe nanocrystal rods/poly(3-hexylthiophene) composite photovoltaic devices. Advanced Materials 1999;11(11):923-927.

[7] Nazzal AY, Qu L, Peng X, Xiao M. Photoactivated CdSe nanocrystals as nanosensors for gases. Nano Letters 2003;3(6):819-822.

[8] De Bastida G, Arregui FJ, Goicoechea J, Matias IR. Quantum dots-based optical fiber temperature sensors fabricated by layer-by-layer. IEEE Sensors Journal 2006;6(6):1378-1379.

[9] Murray CB, Norris DJ, Bawendi MG. Synthesis and characterization of nearly monodisperse CdE(E= S, Se, Te) semiconductor nanocrystallites. SPIE Milestone Series 2005;180:43-52.

[10] Hines MA, Guyot-Sionnest P. Synthesis and characterization of strongly luminescing ZnS-capped CdSe nanocrystals. J Phys Chem 1996;100(2):468-471.

[11] Peng ZA, Peng X. Formation of high-quality CdTe, CdSe, and CdS nanocrystals using CdO as precursor. J Am Chem Soc 2001;123(1):183-184.

[12] Gerbec JA, Magana D, Washington A, Strouse GF. Microwave-enhanced reaction rates for nanoparticle synthesis. J Am Chem Soc 2005;127(45):15791-15800.

[13] Ziegler J, Merkulov A, Grabolle M, Resch-Genger U, Nann T. High-quality ZnS shells for CdSe nanoparticles: rapid microwave synthesis. Langmuir 2007;23(14):7751-7759.

[14] Lee J, Kotov NA. Thermometer design at the nanoscale. Nano Today 2007;2(1):48-51.

[15] Walker GW, Sundar VC, Rudzinski CM, Wun AW, Bawendi MG, Nocera DG. Quantum-dot optical temperature probes. Applied Physics Letters 2003;83:3555-3557.

[16] Li J, Hong X, Liu Y, Li D, Wang YW, Li JH, et al. Highly photoluminescent CdTe/Poly(N-isopropylacrylamide) temperature-sensitive gels. Advanced Materials 2005;17(2):163-166.

[17] Schild HG. Poly(N-isopropylacrylamide): experiment, theory and application. Progress in Polymer Science 1992;17(2):163-249.

[18] Uehara M, Nakamura H, Maeda H. Synthesis of ZnS/CdSe/ZnS quantum dot quantum well in a micro reactor. Berlin: Springer; 2007.

[19] Yang W, Li W, Dou H, Sun K. Hydrothermal synthesis for high-quality CdTe quantum dots capped by cysteamine. Materials Letters 2008;62(17-18):2564-2566.

[20] Boatman EM, Lisensky GC, Nordell KJ. A safer, easier, faster synthesis for CdSe quantum dot nanocrystals. Journal of Chemical Education 2005;82(11):3.

[21] Williams JV, Adams CN, Kotov NA, Savage PE. Hydrothermal synthesis of CdSe nanoparticles. Industrial & Engineering Chemistry Research 2007;46(13):4358-4362.

[22] Yu WW, Peng X. Formation of high-quality cds and other II- VI semiconductor nanocrystals in noncoordinating solvents: tunable reactivity of monomers. Angewandte Chemie (International ed Print) 2002;41(13):2368-2371.

[23] Ferguson JD. Focused™ microwave instrumentation from CEM Corporation. Molecular Diversity 2003;7(2):281-286.

[24] Gedye R, Smith F, Westaway K, Ali H, Baldisera L, Laberge L, et al. The use of microwave ovens for rapid organic synthesis. Tetrahedron Letters 1986;27(3):279-282.

[25] Giguere RJ, Bray TL, Duncan SM, Majetich G. Application of commercial microwave ovens to organic synthesis. Tetrahedron Letters 1986;27(41):4945-4948.

[26] Loones KTJ, Maes BUW, Rombouts G, Hostyn S, Diels G. Microwave-assisted organic synthesis: scale-up of palladium-catalyzed aminations using single-mode and multi-mode microwave equipment. Tetrahedron 2005;61(43):10338-10348.

[27] Dai Q, Song Y, Li D, Chen H, Kan S, Zou B, et al. Temperature dependence of band gap in CdSe nanocrystals. Chemical Physics Letters 2007;439(1-3):65-68.

[28] Dimitrov I, Trzebicka B, Müller AHE, Dworak A, Tsvetanov CB. Thermosensitive water-soluble copolymers with doubly responsive reversibly interacting entities. Progress in Polymer Science 2007;32(11):1275-1343.

[29] Heskins M, Guillet JE. Solution properties of poly(N-isopropylacrylamide). Journal of Macromolecular Science, Part A 1968;2(8):1441-1455.

[30] Yamato M, Akiyama Y, Kobayashi J, Yang J, Kikuchi A, Okano T. Temperature-responsive cell culture surfaces for regenerative medicine with cell sheet engineering. Progress in Polymer Science 2007;32(8-9):1123-1133.

[31] Hou Y, Matthews AR, Smitherman AM, Bulick AS, Hahn MS, Hou H, et al. Thermoresponsive nanocomposite hydrogels with cell-releasing behavior. Biomaterials 2008;29(22):3175-3184.

[32] Kim YH, Bae YH, Kim SW. pH/temperature-sensitive polymers for macromolecular drug loading and release. Journal of Controlled Release 1994;28(1-3):143-152.

[33] Xu S, Zhang J, Paquet C, Lin Y, Kumacheva E. From hybrid microgels to photonic crystals. Advanced Functional Materials 2003;13(6):468-472.

[34] Gong Y, Gao M, Wang D, Mohwald H. Incorporating fluorescent CdTe nanocrystals into a hydrogel via hydrogen bonding: toward fluorescent microspheres with temperature-responsive properties. Chem Mater 2005;17(10):2648-2653.

[35] Medintz IL, Clapp AR, Mattoussi H, Goldman ER, Fisher B, Mauro JM. Self-assembled nanoscale biosensors based on quantum dot FRET donors. Nature Materials 2003;2(9):630-638.

[36] Nann T. Phase-transfer of CdSe@ ZnS quantum dots using amphiphilic hyperbranched polyethylenimine. Chemical Communications 2005;2005(13):1735-1736.

[37] Singh D, Kuckling D, Choudhary V, Adler HJ, Koul V. Synthesis and characterization of poly(N-isopropylacrylamide) films by photopolymerization. Polymers for Advanced Technologies 2006;17(3):186-192.

[38] Yu WW, Qu L, Guo W, Peng X. Experimental determination of the extinction coefficient of CdTe, CdSe, and CdS nanocrystals. Chem Mater 2003;15(14):2854-2860.

[39] Zhang BB, Liu XH, Li DN, Tian H, Ma GP, Chang J. Preparation of multi-color quantum dots and its application to immunohistochemical analysis. Chinese Science Bulletin 2008;53(13):2077-2083.

[40] Lu1ã W, Umezu I, Sugimura A. Evolution of energy transfer process between quantum dots of two different sizes during the evaporation of solvent. Japanese Journal of Applied Physics 2008;47(8):6592-6595.

[41] Kagan CR, Murray CB, Bawendi MG. Long-range resonance transfer of electronic excitations in close-packed CdSe quantum-dot solids. Physical Review B 1996;54(12):8633-8643.

[42] Mohs AM, Duan H, Kairdolf BA, Smith AM, Nie S. Proton-resistant quantum dots: stability in gastrointestinal fluids and implications for oral delivery of nanoparticle agents. Nano Research 2009;2(6):500-508.

VITA

Name:	Ameet Rajkumar Juriani
Address:	337 Zachry Engineering Center 3120 TAMU College Station, TX 77843-3120
E-mail Address:	ameet602@gmail.com
Education:	B.E., Biomedical Engineering, Mumbai University, June 2006 M.S., Biomedical Engineering, Texas A&M University, May 2010